WAVE PROPAGATION IN A RANDOM MEDIUM

R. W. Lee and J. C. Harp

Stanford Electronics Laboratories
Stanford University

ABSTRACT

A simple technique has been used to derive statistical characterizations of the perturbations imposed upon a wave (plane, spherical or beamed) propagating through a random medium. The method is essentially physical rather than mathematical, and is probably equivalent to the Rytov method. The limitations of the method are discussed in some detail; in general they are restrictive only for optical paths longer than a few hundred meters, and for paths at the lower microwave frequencies. Situations treated include arbitrary path geometries, finite transmitting and receiving apertures, and anisotropic media. Results include, in addition to the usual statistical quantities, time-lagged functions, mixed functions involving amplitude and phase fluctuations, angle-of-arrival covariances, frequency covariances, and other higher-order quantities.

1. INTRODUCTION

An increasing amount of interest has been focused in recent years upon the problem of electromagnetic wave propagation in media whose properties are random functions of space and time. The atmosphere of the earth is such a medium, and this interest has been aroused both by technological pressure for more efficient utilization of the radio-through-optical spectrum, and by the recognition that the effects produced by the atmosphere upon waves propagating through it are useful measures of the nature of the atmosphere. In order that perturbations observed on propagated waves may be interpreted in terms of atmospheric parameters, it is necessary to evolve a sound theoretical framework, based upon a realistic model of the atmosphere. The atmospheric model used must be amenable to the necessary mathematical operations of the theoretical analysis, but must at the same time possess sufficient degrees of freedom to represent adequately the actual random medium.

While this last requirement has not always been met in attempts to develop the theory of propagation through random media, notable progress has been made. The work of Tatarski (1961) is a satisfactory basis for plane-wave situations, and that of Schmeltzer (1967) extends the work to spherical-wave, finite-aperture situations. Both authors use the Rytov method, developed 30 years ago in connection with work on the diffraction of light by ultrasonic beams. Considerable discussion has attended the use of this method, primarily concerning the range of validity of the approximation. In particular, the sufficiency conditions obtained in the mathematical approach (that the aggregate of the perturbations on the wave be much less than the magnitude of the wave, and that all refractive perturbations be large compared to a wavelength) have been considered by some to be unnecessarily severe. If the requirement that all refractive perturbations be much larger than a wavelength is taken at face value, application of these theories is restricted to wavelengths of less than about 1 mm, since it is known that inhomogeneities at least as small as a few mm are present in the atmosphere.

In the development that follows a very simple technique will be used to obtain a wide variety of statistical characterizations of the perturbations produced by a random medium upon a wave propagating through it. The method is basically physical and geometrical, rather than mathematical; as a result, when approximations are made, they arise in a physical context, making it possible to assess more easily the implications of the approximations.

Briefly, the technique consists of resolving the 3-dimensional refractivity field of the medium into thin slabs perpendicular to the propagation path, and further resolving the 2-dimensional refractivity field within a slab into Fourier components of varying wavenumber and angle in polar coordinates. The effect produced upon the wave by one of these Fourier components is then determined, a simple matter because the component acts exactly like a phase diffraction-grating. The resolution is then retraced, and perturbations produced by Fourier components of differing wavenumber, angle and position along the path are summed statistically.

The resulting solution is composed of three multiplicative terms: the power spectrum of the refractive irregularities, a term relating the fluctuations at one point in the receiving plane to those at another point, and a term which is a measure of the relative efficiency of an irregularity of a given size, located at a given position along the transmission path, in producing perturbations at the receiver. This latter term is generally referred to as a "filter function," serving as it does to weight selectively the spectrum of refractive irregularities.

This method is used in Sections 2 and 3 to obtain spatial covariance- and structure-functions for the plane- and spherical-wave situations; a discussion of the region of validity of this development is given in Section 4. The theory is extended in succeeding sections to include anisotropic media (Section 5), temporal quantities (Section 6), additional higher statistical functions (Section 7), finite transmitting and receiving apertures (Section 8), and non-transparent media (Section 9). Section 10 is devoted to examples of "filter functions," just described. These functions depend upon the path geometry and the measurement being made, and are quite important factors in the interpretation of measurements in terms of atmospheric parameters. Finally, Section 11 consists of a discus-

sion of the techniques available for extracting from experimental measurements information about the medium—information concerning not only quantities averaged over the transmission path, but concerning the spatial distribution of such quantities as well.

2. PROPAGATION OF AN INFINITE PLANE-WAVE

A plane-wave propagating in the z-direction with wavenumber k exp(-ikz) is incident upon an infinite slab bounded by the planes z = r and z = r + dz. The slab imposes upon the wave a phase perturbation which is sinusoidal in x, and of peak magnitude kadz:

$$\Delta\phi = \text{kadz cos } (u(x+b)) \tag{2.1}$$

where u is the wavenumber of the perturbation, and ub is the phase of the perturbation at the z-axis. At this point we shall make the assumption that $k \gg |\bar{u}|$ for all wavenumbers in the refractivity spectrum (see Figure 2.1).

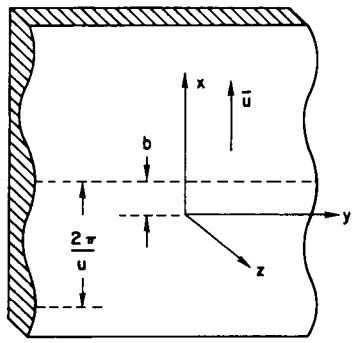

Figure 2.1

Upon exiting from the slab the incident wave is then

$$\exp(-ikr) \cdot \exp\{-ika\ dz \cos(u(x+b))\}. \tag{2.2}$$

Assuming that the perturbation is small ($ka\,dz \ll 1$), (1.2) may be written

$$\begin{aligned} &\exp(-ikr)\{1-ika\ dz \cos(u(x+b))\} \\ &= \exp(-ikr) - \frac{ika\ dz}{2}\exp(-ikr)\exp(iu(x+b)) \\ &\quad - \frac{ika\ dz}{2}\exp(-ikr)\exp(-iu(x+b)). \end{aligned} \tag{2.3}$$

The first term of (2.3) represents the original wave, undiminished in the weak-scattering approximation. The second term represents another plane-wave, propagating at an angle θ with respect to the z-axis and an angle γ with respect to the x-axis, where

$$\gamma = \arccos(u/k)$$

$$\theta = \arccos\left(\sqrt{1-u^2/k^2}\right)$$

The projection of $\bar{k}$ on the z-axis is $k \cos \theta = \sqrt{k^2 - u^2}$, the effective wavenumber k' of the scattered wave. The wave is, of course, invariant in y. The third term of (2.3) represents another plane-wave, the mirror image of the second wave as reflected in the plane $x=b$ (see Figure 2.2). At the plane $z=L$, these three become:

$$\begin{aligned} &\exp(-ikr)\exp(ik(L-r)) \\ &\exp(-ikr)(-ikadz/2)\exp\{-ik'(L-r)-iu(x+b)\} \\ &\exp(-ikr)(-ikadz/2)\exp\{-ik'(L-r)+iu(x+b)\} \end{aligned} \tag{2.4}$$

The resulting field dE_t at the plane $z = L$ is the sum of these three waves.

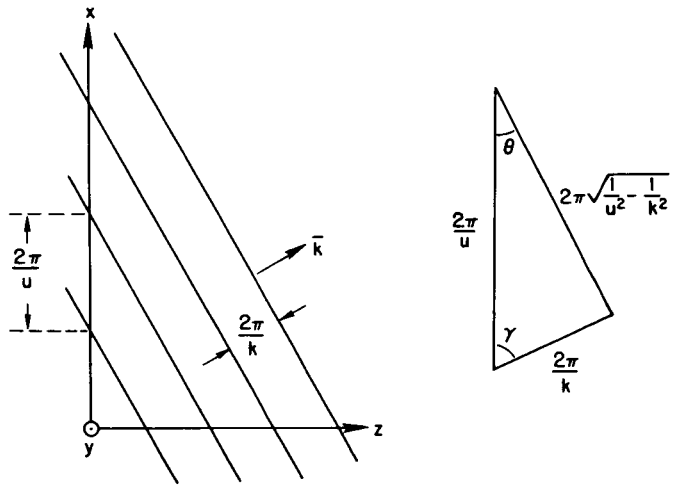

Figure 2.2

Dropping the common phase term exp (-ikr) and setting $L - r = s$, the sum becomes

$$\begin{aligned} dE_t &= \exp(-iks) - (ikads/2)\exp\{-ik's-iu(x+b)\} \\ &\quad - (ikads/2)\exp\{-ik's+iu(x+b)\} \\ &= \exp(-iks) - ikads \cdot \exp(-ik's)\cos(u(x+b)) \end{aligned} \tag{2.5}$$

Factoring and dropping the phase term exp (-iks),

$$dE_t = 1 - ika \cdot ds \cdot \exp\{-is(k'-k)\}\cos(u(x+b)). \tag{2.6}$$

The observed perturbation of the field in the plane $z=L$ is the difference of the magnitudes of the perturbed and unperturbed fields.

$$\begin{aligned} dP_a &= |dE_t| - 1 = [\mathcal{R}^2(dE_t) + \mathcal{I}^2(dE_t)]^{1/2} - 1 \\ &= ka \cdot ds \cdot \cos[u(x+b)] \cdot \sin[s(k'-k)]. \end{aligned} \tag{2.7}$$

Terms in a^2 are neglected. Note that the perturbation of the field is sinusoidal in x, displaced in phase by ub, with period $2\pi/u$; that is, the field perturbation is a projection on the plane $z=L$ of the perturbing sinusoidal lens.

The perturbation of the phase front in the plane $z=L$ is

$$\begin{aligned} dP_p &= \tan^{-1}[\mathcal{I}(dE_t)/\mathcal{R}(dE_t)] \\ &= ka \cdot ds \cdot \cos[u(x+b)]\cos[s(k'-k)]. \end{aligned} \tag{2.8}$$

The spatial-covariance function C(d) of the field perturbations is the ensemble average of the products of all perturbations observed at a point x_1 with all perturbations at another point x_2. Assuming that the average product of perturbations of differing wavenumber $\bar{u}$ is zero (since if the refractivity field is random, the Fourier components of that field are uncorrelated) there remain the cross-products resulting from a given wavenumber $\bar{u}$ at two points s_1 and s_2 on the path. The sum of such cross-products for all s_1 and s_2 is

$$dC_a(d) = k^2 \int_0^L \sin(s_1(k'-k)) \int_0^L \sin(s_2(k'-k)). \tag{2.9}$$

$$\langle a(u,s_1)\cos(u(x_1+b_1)) \cdot a(u,s_2)\cos(u(x_2+b_2))\rangle \, ds_1 ds_2.$$

We see that the quantity within the $\langle\rangle$ brackets is simply the correlation between parallel slabs containing the same u and separated by s_1-x_1). This is just the average product of two expressions

$$\langle [d\Psi_r(u,s_1)\exp(iux_1) + d\Psi_r(-u,s_1)\exp(-iux_1)]. \tag{2.10}$$

$$[d\Psi_r(u,s_2)\exp(iux_2) + d\Psi_r(-u,s_2)\exp(-iux_2)]\rangle.$$

The integral (2.9) may be simplified to:

$$dC_a(d) = 2k^2 \int_0^L \sin(s_1(k'-k)) \int_0^L \sin(s_2(k'-k)). \tag{2.11}$$

$$\cos(u(x_1-x_2))\, F_r(u,s_1-s_2)\, ds_1 ds_2.$$

This integral has been handled by Tatarski (1961, Chapter 8) for the case $k \gg u$, with the result:

$$dCa(d) = 4\pi k^2 \int_0^L \Phi(u) \sin^2 \frac{u^2 s}{2k} \, ds \cos(u(x_1-x_2)), \tag{2.12}$$

where $s = (s_1 + s_2/2)$ and $\Phi(u)$ is the three-dimensional power spectrum of the turbulence, $\Phi(u_x,u_y,u_z)$, evaluated at $u_z = 0$.

The total covariance $C_a(d)$ is the integral of $dC_a(d)$ over all wavenumbers $\bar{u}$.

$$C_a(d) = 4\pi k^2 \int_0^\infty \int_0^L \Phi(u) \cdot \sin^2\left(\frac{u^2 s}{2k}\right) \cos(u(x_1-x_2)) \, ds d\bar{u}. \tag{2.13}$$

Taking $d\bar{u} = u \cdot du \cdot d\phi$, noting that the projection of the receiver separation d upon $\bar{u}$, $d\cdot\cos\phi$, is the difference $(x_1 - x_2)$ of the x-coordinates of the two receivers, and limiting the integration in $\bar{u}$ such that $|\bar{u}| \leq k$,

$$C_a(d) = 4\pi k^2 \int_0^k du \int_0^L ds \int_0^{\pi} d\phi \; u\Phi(u) \cos(du\cdot\cos\phi)\sin^2[u^2 s/2k] \qquad (2.14)$$

Performing the integration in ϕ, assuming $\Phi(u)$ to be independent of ϕ:

$$C_a(d) = 4\pi^2 k^2 \int_0^k du \int_0^L ds \; u\Phi(u) J_o(du) \sin^2(u^2 s/2k). \qquad (2.15)$$

This is the form given by Tatarski (1961, p. 168). If $\Phi(u)$ is independent of s, (2.13) reduces to

$$C_a(d) = 2\pi^2 k^2 L \int_0^L du \; u\Phi(u) \, Jo(du) \left[1 - \frac{k}{u^2 L} \sin \frac{u^2 L}{k}\right] . \qquad (2.16)$$

Amplitude variance is obtained by setting d = O.

$$C_a(O) = 4\pi^2 k^2 L \int_0^k du \int_0^L ds u\Phi(u) \sin^2(u^2 s/2k). \qquad (2.17)$$

Phase covariance follows from (2.8) by simply replacing the sin $[s(k' - k)]$ term by cos $[s(k' - k)]$ in the foregoing development. For example,

$$C_p(d) = 4\pi^2 k^2 \int_0^k du \int_0^L ds \; u\Phi(u) \, Jo(du) \cos^2 [u^2 s/2k] . \qquad (2.18)$$

Again, if $\Phi(u)$ is independent of s, this reduces to

$$C_p(d) = 2\pi^2 k^2 L \int_0^k du \; u\Phi(u) \, Jo(du) \left(1 + \frac{k}{u^2 L} \sin \frac{u^2 L}{k}\right). \qquad (2.19)$$

The latter is the form given by Tatarski (1961, p. 143). Structure-functions follow from the definition

$$D_i(d) = 2(C_i(O) - C_i(d)).$$

Thus,

$$D_a(d) = 8\pi^2 k^2 \int_0^k du \int_0^L ds \; u\Phi(u) \; [1 - Jo(du)] \sin^2 (u^2 s/2k). \qquad (2.20)$$

$$D_p(d) = 8\pi^2 k^2 \int_0^k du \int_0^L ds \; u\Phi(u) \; [1 - Jo(du)] \cos^2 (u^2 s/2k). \qquad (2.21)$$

and the wave structure-function,

$$D(d) = D_a(d) + D_p(d) = 8\pi^2 k^2 \int_0^k du \int_0^L ds\, u\Phi(u)\,[1-Jo(du)] \tag{2.22}$$

$$= 8\pi^2 k^2 L \int_0^k du\, u\Phi(u)\,[1-Jo(du)], \Phi(u) \neq f(s).$$

3. PROPAGATION OF A SPHERICAL-WAVE

The development of the spherical-wave case closely follows that of the preceding section. A spherical-wave expanding from the origin at (O,O,O), with wavenumber k, has near the z-axis at z = s the magnitude

$$\frac{L}{s} \exp\left(-ik\sqrt{s^2 + x^2 + y^2}\right).$$

The magnitude is normalized to unity at z = L, the plane of the receiving points. This wave is incident upon an infinite slab in the plane z = s, of thickness dz. As in the plane wave case, the slab imposes upon the wave a perturbation in phase, sinusoidal in x (cf. (2.1) and Figure 2.1), of peak magnitude k a dz:

$$d_{phase} = k\, a\, dz \cos(u\,(x + b)) \tag{3.1}$$

where u is the wavenumber of the perturbation, and b is the phase of the perturbation at the z-axis. Upon exiting from the slab the incident wave becomes

$$\frac{L}{s} \exp\left(-ik\sqrt{s^2 + x^2 + y^2}\right) \exp(-ik\, a\, dz \cos(u\,(x + b))). \tag{3.2}$$

Since the perturbation is assumed to be small (k a dz $\ll$ 1), (3.2) may be written

$$\frac{L}{s} \exp\left(-ik\sqrt{s^2 + x^2 + y^2}\right)(1 - ik\, a\, dz \cos(u\,(x + b))) \tag{3.3}$$

$$= \frac{L}{s} \exp\left(-ik\sqrt{s^2 + x^2 + y^2}\right) - \frac{ikaLdz}{2s} \exp\left(-ik\sqrt{s^2 + x^2 + y^2}\right) \exp$$

$$- \frac{ikaLdz}{2s} \exp\left(-ik\sqrt{s^2 + x^2 + y^2}\right) \exp(-iu(x + b))$$

Near the z-axis (x,y $\ll$ s), (3.3) may be written

$$\frac{L}{s} \exp\left(-ik\sqrt{s^2 + x^2 + y^2}\right) - \frac{idaLdz}{2s} \exp\left[-ik\left(s + \frac{x^2}{2s} + \frac{y^2}{2s}\right)\right] \exp[-iu(x + b)] \tag{3.4}$$

$$- \frac{ikaLdz}{2s} \exp\left[-ik\left(s + \frac{x^2}{2s} + \frac{y^2}{2s}\right)\right] \exp[-iu(x + b)]$$

$$= \frac{L}{s} \exp\left[-ik\sqrt{s^2 + x^2 + y^2}\right] - \frac{ikaLdz}{2s} \exp(iub) \exp\left[-ik\left(s + \frac{y^2}{2s} + \frac{x^2}{2s} - \frac{ux}{k}\right)\right]$$

$$- \frac{ikaLdz}{2s} \exp(iub) \exp\left[-ik\left(s + \frac{y^2}{2s} + \frac{x^2}{2s} + \frac{ux}{k}\right)\right]$$

Completing the square of the x-terms, and factoring the remainder:

$$\frac{L}{s}\exp\left[-ik\sqrt{s^2+x^2+y^2}\right] \tag{3.5}$$

$$-\frac{ikaLdz}{2s}\exp(iub)\exp\left[\frac{iu^2s}{2k}\right]\exp\left(-ik\left[s+\frac{y^2}{2s}+\frac{[x-us/k]^2}{2s}\right]\right)$$

$$-\frac{ikaLdz}{2s}\exp(-iub)\exp\left[\frac{iu^2s}{2k}\right]\exp\left(-ik\left[s+\frac{y^2}{2s}+\frac{[x=us/k]^2}{2s}\right]\right)$$

The first term of (3.5) is the original spherical-wave, undiminished in the weak-scattering approximation. The next two terms represent two additional spherical waves, originating from the points [us/k, O, O] and [-us/k, O, O], differing in amplitude from the original wave by the factor

$$ka\frac{dz}{2},$$

and in phase by the factor $\exp \pm (iub)\exp[iu^2s/2k]$. Note that it is required that

$$2s^2 >> \left(x+\frac{us}{k}\right)^2.$$

This is satisfied if x is small and $k >> u$. In the plane $z = L$ the sum of these three spherical-waves is

$$dE_t = \exp\left(-ik\left(L+\frac{x^2}{2L}+\frac{y^2}{2L}\right)\right) \tag{3.6}$$

$$-\frac{ikadz}{2}\exp(iub)\exp\left(\frac{iu^2s}{2k}\right)\exp\left[-ik\left(L+\frac{y^2}{2L}+\frac{(x-us/k)^2}{2L}\right)\right]$$

$$-\frac{idadz}{2}\exp(-iub)\exp\left(\frac{iu^2s}{2k}\right)\exp\left[-ik\left(L+\frac{y^2}{2L}+\frac{(x+us/k)^2}{2L}\right)\right]$$

Factoring and dropping the common phase term $\exp[-ik(L + y^2/2L)]$,

$$dE_t = \exp\left[\frac{-ikx^2}{2L}\right]-\frac{ikadz}{2}\exp\left[\frac{iu^2s}{2K}\right]\left(\exp(iub)\exp\left(\frac{-ik}{2L}\left[x-\frac{us}{k}\right]^2\right)\right. \tag{3.7}$$

$$\left.+\exp(-iub)\exp\left(\frac{-ik}{2L}\left[x+\frac{us}{k}\right]^2\right)\right)$$

Dropping another common phase factor $\exp[-ikx^2/2L]$ and combining terms,

$$dE_t = 1-\frac{ikadz}{2}\exp\left[\frac{iu^2s}{2K}\right]\exp\left[\frac{-iu^2s^2}{2kL}\right]\left(\exp(iub)\exp\left[\frac{iuxs}{L}\right]+\right. \tag{3.8}$$

$$\left.\exp(-iub)\exp\left[\frac{-iuxs}{L}\right]\right)$$

$$= 1-ikadz\exp\left[\frac{iu^2s(L-s)}{2kL}\right]\cos\left[u\left(\frac{xs}{L}+b\right)\right].$$

The observed field perturbation at (x,y,L) is the difference of the magnitudes of the perturbed and unperturbed fields

$$dPa = |dE_t| - 1 = \left[\mathcal{R}^2 (dE_t) + \mathcal{I}^2 (dE_t)\right]^{1/2} - 1 \tag{3.9}$$

$$= kadz \sin\left[\frac{u^2 s(L-s)}{2kL}\right] \cos\left[u\left(\frac{xs}{L} + b\right)\right].$$

Terms in a^2 are neglected. As in the plane-wave case, the perturbation of the field is sinusoidal in x (and independent of the y-coordinate of the receiver), but the period is $2\pi L/su$ (rather than $2\pi/u$). That is, the period of the perturbation of the field in the plane z = L is the projection of the period of the perturber in the plane z = s.

The perturbation of the phasefront in the plane z = L is

$$dP_p = \tan^{-1}\left[\frac{\mathcal{I}\, dE_t}{\mathcal{R}\, dE_t}\right] \tag{3.10}$$

$$= kadz \cos\left[\frac{u^2 s\,(L-s)}{2kL}\right] \cos\left[u\left(\frac{xs}{L} + b\right)\right].$$

The spatial-covariance function of amplitude $dC_a(d)$ becomes (cf. (2.9)):

$$dC_a(d) = k^2 \int_0^L \sin\left[\frac{u^2 s_1(L-s_1)}{2kL}\right] \int_0^L \sin\left[\frac{u^2 s_2(L-s_2)}{2kL}\right] \tag{3.11}$$

$$\cdot \left\langle \left\{a(u,s_1) \cos\left[u\left(\frac{x_1 s_1}{L} + b_1\right)\right]\right\} \cdot \left\{a(u,s_2) \cos\left[u\left(\frac{x_2 s_2}{L} + b_2\right)\right]\right\} \right\rangle .$$

Once again, as in Section 2, the $\langle\,\rangle$ term is identifiable with equation (I.6) of Appendix I. Following the development in Section 2, with the one additional assumption that $L >> \lambda$, we obtain an expression for (3.11):

$$dC_a(d) = 4\pi k^2 \int_0^L \Phi(u) \sin^2\left[\frac{u^2 s(L-s)}{2kL}\right] \cos\left[u\frac{(x_1 x_2)}{L} s\right] ds. \tag{3.12}$$

Integrating this expression over all $\bar{u}$ as was done in Section 2, we obtain:

$$C_a(d) = 4\pi^2 k^2 \int_0^\infty \int_0^L u\Phi(u)\, J_o\left(\frac{dus}{L}\right) \sin^2\left[\frac{u^2 s\,(L-s)}{2kL}\right] dsdu. \tag{3.13}$$

This is the form given by Schmeltzer (1967, p. 354) as used by Fried (1966, p. 1381). In the case of d = 0 (variance), (3.13) was first derived by Tatarski (1961, p. 183).

If the refractive fluctuations are finite only over the range L - H < s < L, the covariance becomes

$$C_a(d) = 4\pi^2 k^2 \int_0^k du \int_{L-H}^{L} ds\, u\Phi(u)\, Jo\left[\frac{dsu}{L}\right] \sin^2\left[\frac{u^2 s(L-s)}{2kL}\right] \tag{3.14}$$

Making L arbitrarily large (removing the transmitter to infinity), $\frac{s}{L} \to 1$ over the range of integration, and

$$C_a(d) = 4\pi^2 k^2 \int_0^k du \int_{L-H}^{L} ds\, u\Phi(u)\, Jo(du) \sin^2\left[\frac{u^2(L-s)}{2k}\right] \tag{3.15}$$

Making the substitution h = L - s, dh = -ds,

$$C_a(d) = 4\pi^2 k^2 \int_0^k du \int_0^H dh\, u\Phi(u)\, Jo(du) \sin^2\left[\frac{u^2 h}{2k}\right] \tag{3.16}$$

which is the plane-wave result (2.13).

Phase-covariance follows from (3.10), simply by replacing the $\sin^2()$ term in (3.13) by $\cos^2()$:

$$C_p(d) = 4\pi^2 k^2 \int_0^k du \int_0^L ds\, u\Phi(u)\, Jo\left[\frac{dsu}{L}\right] \cos^2\left[\frac{u^2 s(L-s)}{2kL}\right] \tag{3.17}$$

Structure functions (cf. (2.18), (2.19), and (2.20)) are:

$$D_a(d) = 8\pi^2 k^2 \int_0^k du \int_0^L ds\, u\Phi(u) \left(1 - Jo\left[\frac{dsu}{L}\right]\right) \sin^2\left[\frac{u^2 s(L-s)}{2kL}\right] \tag{3.18}$$

$$D_p(d) = 8\pi^2 k^2 \int_0^k du \int_0^L ds\, u\Phi(u) \left(1 - Jo\left[\frac{dsu}{L}\right]\right) \cos^2\left[\frac{u^2 s(L-s)}{2kL}\right] \tag{3.19}$$

$$D(d) = 8\pi^2 k^2 \int_0^k du \int_0^L ds\, u\Phi(u) \left(1 - Jo\left[\frac{dsu}{L}\right]\right) \tag{3.20}$$

The amplitude covariance function (3.13), evaluated for several cases, is shown in Figure 3.1. The refractivity spectrum $\Phi(u)$ assumed in the evaluations was a simple power-law spectrum, with an exponent of -11/3 (Kolmogorov) or -4. Other parameters used were L = 28 km, k = 716 (35 GHz). The covariance functions are normalized by dividing by $C_a(O)$. The central pair of curves in Figure 3.1 is for the normal spherical-wave situation, a single transmitter and two spaced receivers separated by d (0 to 20 m). A similar curve for the Kolmogorov spectrum has been published by Fried (1967, p. 178).

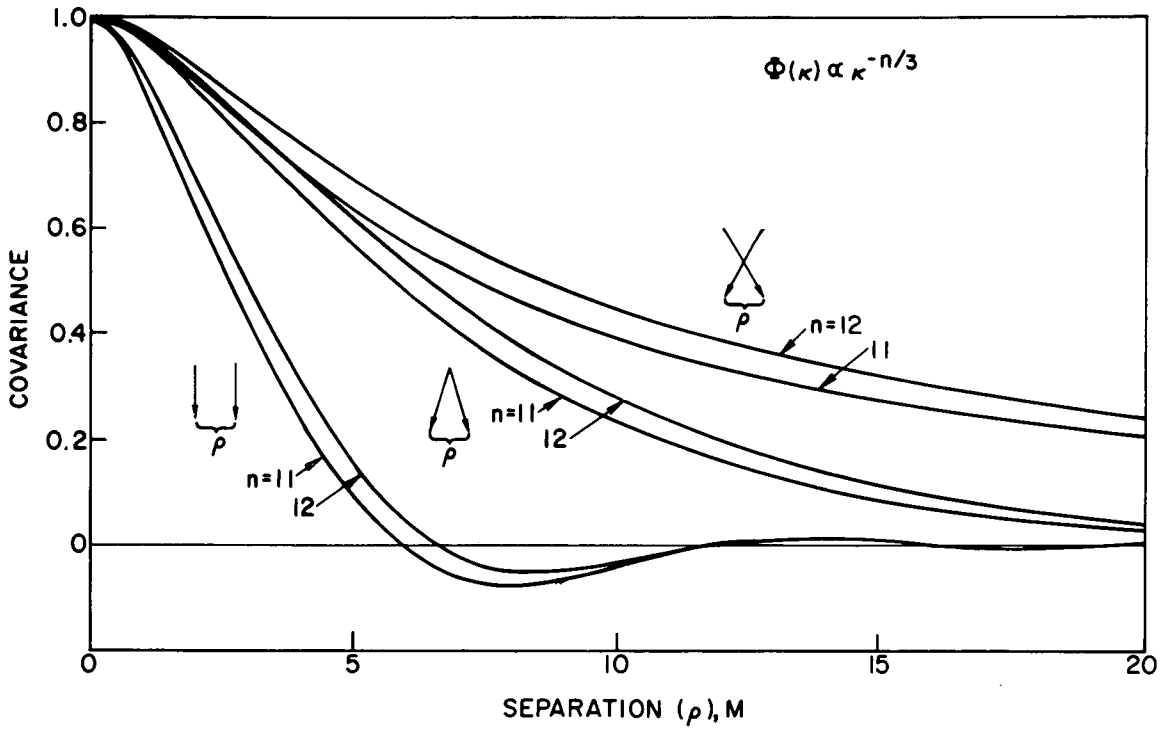

Figure 3.1. Amplitude covariance as a function of path separation ρ, for three path geometries.

The other two pairs of curves in Figure 3.1 are for crossed- and parallel-path geometries; that is, the two receivers are coupled to two separated transmitters, each transmitter-receiver system being independent of the other. To treat such geometries theoretically, it is only necessary to recognize that the quantity ds/L in (3.13) represents the separation between the two paths connecting the transmitter to the receivers. In the parallel-path situation (viz. the plane-wave case) this separation is constant along s, and the Bessel function in (3.13) becomes Jo(du). In the crossed-path case, it becomes

$$\mathrm{Jo}\left[\frac{\mathrm{du(L-2s)}}{\mathrm{L}}\right] .$$

Another family of theoretical evaluations of (3.13) is shown in Figure 3.2. The same path parameters are used, with additional curves for other refractivity spectra plotted. Also shown in the figure are experimental results obtained over a path described by Lee and Waterman (1966, pp. 454-458). The data represent 32-hour means, with 10th and 90th percentiles of 100-sec measurements. The mean values follow the theoretical curves well as to form, although the Kolmogorov spectrum does not give the best fit.

Evaluation of the phase structure function (3.19) has been performed by Fried (1967, p. 179). For a Kolmogorov refractivity spectrum, over the region in separation d of interest here the structure function follows a power-law with a slope of 5/3. Experimental measurements of the phase structure function, over the path just mentioned, are plotted in Figure 3.3. The data represent 100-sec samples, taken at random over a two day period. Differences in magnitude among the curves reflect variations in the magnitude of the refractivity spectrum (that is, changes in C_n^2). The curves shown in Figure 3.3 approximate a 5/3 slope.

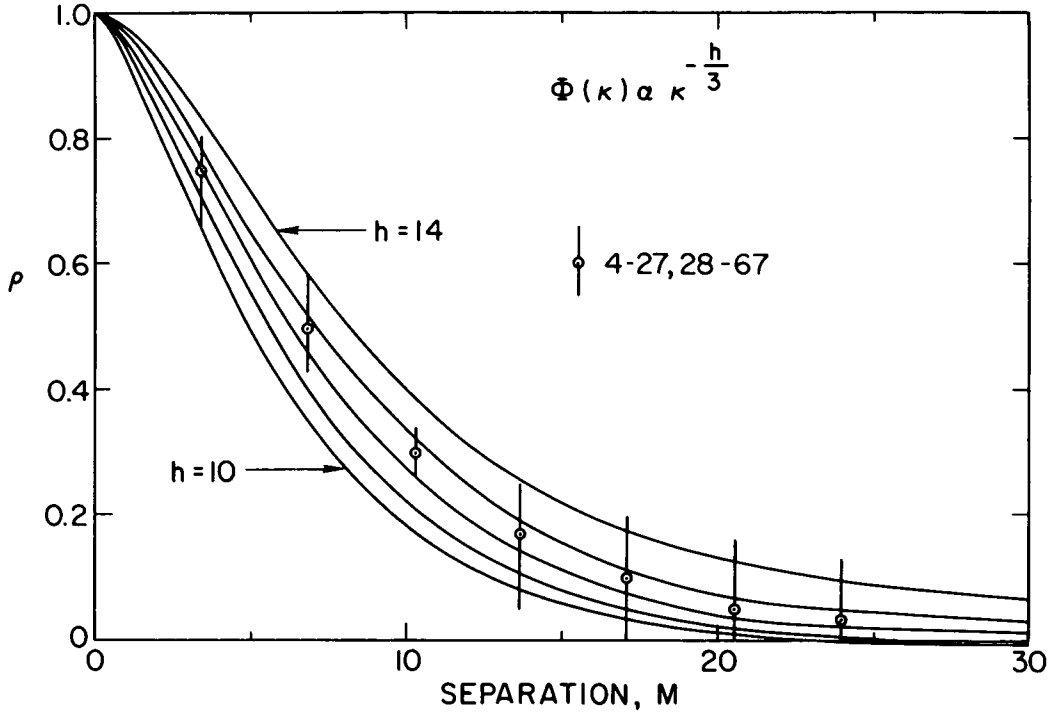

Figure 3.2. Amplitude covariance functions for different spectra $\Phi(u)$, with experimental data.

4. ON THE LIMITATIONS OF THE THEORY

Whether or not this theoretical framework (or any theory, for that matter) is suitable for application to a given experimental situation depends upon the validity of two classes of assumptions. The first class involves the accuracy of the assumptions made concerning the parameters of the physical world as introduced into the theory—in this case, the nature of the refractivity field as approximated by a three-dimensional spectrum and associated statistical characterizations. The second class consists of those assumptions (usually called approximations) which arise out of the mathematical necessity, in the process of obtaining mathematically simple (if physically unrealistic) solutions. The preceding theoretical development possesses considerable advantage over more abstract mathematical approaches in this respect, in that approximations of the sort just mentioned arise in a clear physical context, making evaluation of the implications of the approximations relatively simple. An analysis of both classes of assumptions follows, for the development of Sections 2 and 3, with the intent being to obtain not only sufficiency conditions, but necessary conditions for the application of the results.

Without doubt the most important assumption made in the development of the theory is that the scattered energy is small compared with the incident wave. The necessity for this assumption arises for two reasons. Taking the plane-wave development of Section 2 (the same argument holds equally well for the spherical- or beamed-wave cases), this assumption allows the exponential of (2.2) to be expanded into (2.3); this not only makes possible the rest of the development, but carries an important implication as well. That

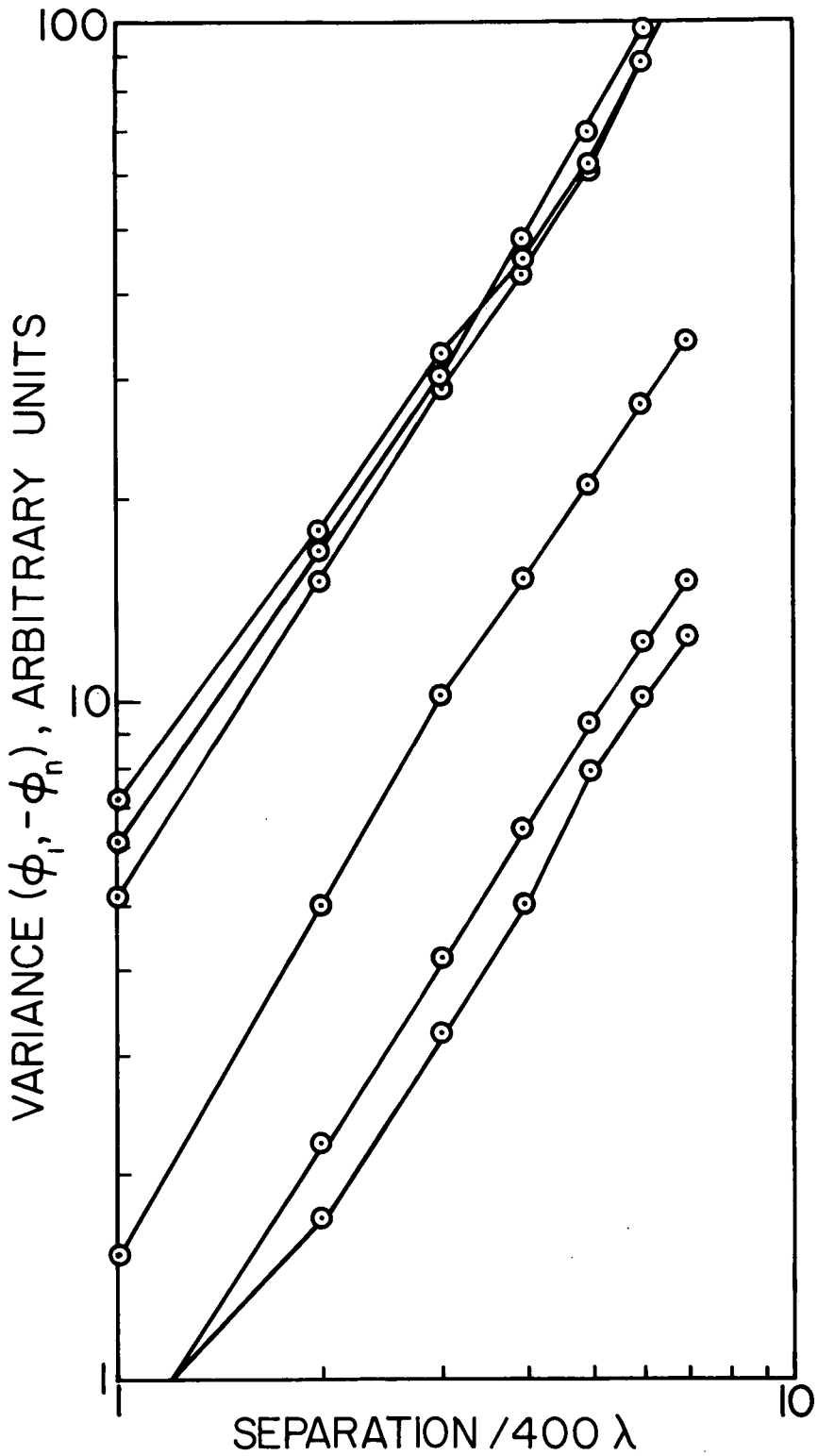

Figure 3.3. Phase structure-functions measured.

is, the expansion used results in the original wave propagating without the loss of energy, while finite energy appears as a scattered component. Clearly energy is not conserved; in actual practice the incident unperturbed wave will decay with distance. The assumption of weak scattering allows two other phenomena to be ignored: multiple scattering (wherein a scattered wave of the type noted in (2.4) can itself be scattered from another slab), and higher order scattering (corresponding to the higher grating orders). The second occasion wherein weak scattering is invoked occurs at the end of the development, when variance is obtained. It is implicit in (2.7) that since the unperturbed field is normalized to unity, the perturbations calculated are ratios of perturbed to unperturbed fields. When the sum of many such perturbations is identified with the covariance, as in (2.15), this identification rests upon the assumption that the sum of the perturbations is less than the unperturbed field. That is, not only must the individual perturbations be small, but their sum must be small. There can be no doubt that the theory breaks down when the variance of the received field approaches unity in terms of the mean field.

It is appropriate to note here that the theory as developed here treats the received field (as normalized by the mean field) rather than the logarithm of the field, as used by Tatarski (1961) and others using the approach of Rytov. Nonetheless, the results obtained here agree in general with the results of log-amplitude treatments. This agreement can be attributed to the weak-scattering assumption for as long as the variance of the received field is appreciably less than unity, there is no significant difference between the logarithm of the field and the departure of the field from unity.

The nature of the limitation imposed by this basic assumption upon application of the theory depends upon the intensity of the refractivity spectrum, as well as upon wavelength and path length. For the lower atmosphere, pathlengths are limited to (typically) hundreds of meters at optical wavelengths, and to hundreds of km at centimeter wavelengths.

It is generally assumed during use of the Rytov method that the wavelength $2\pi/k$ is much smaller than the smallest dielectric irregularity; that is, $k \gg u_{max}$. (4.1)

It is generally agreed that a lower limit on irregularity size exists in the atmosphere (l_0, the "inner scale" of turbulence), and is of the order of millimeters. Taken at face value this assumption limits the use of the theory to wavelengths shorter than a millimeter or so. In order to extend the validity of the theory to longer wavelenghs, it is necessary to consider the effect of wavenumbers u ranging from about k/10 (where k can be considered much greater than u) to infinity. First consider the region u greater than k.

It can be seen from (2.3) that the sinusoidal phase-perturber of Figure 2.1 is equivalent to a sinusoidal amplitude-perturber lagging 90° in phase. The perturbation emerges from the equivalent of a transmission grating, with adjacent "slits" differing in phase by 180° due to the cosine term. The angles defined in Figure 2.2 are simply the grating-lobe angles. With this background, the effect of reducing the grating spacing is evident. As the spacing decreases (corresponding to higher wavenumber u) the grating angles become larger (corresponding to the perturbing wave arriving from farther off path) until, for k = u, they are ±180°. When u exceeds k there are no longer solutions which result in constructive interference for any angle, and, in fact, the effective wavenumber of the emerging perturbation k' becomes imaginary, as can bee seen from the definition.

$$k' = \sqrt{k^2 - u^2}. \tag{4.2}$$

In this situation the additional waves caused by the perturbation (the so-called evanescent waves) do not propagate more than a few wavelengths. Hence the integration in u (cf. (2.15)) may be safely terminated at k, rather than infinity, and no limitation need be imposed upon k. We are left with the region k = u to k >> u. This is the region of wide-angle scattering, scattering which is usually ignored, being removed from mathematical developments by the use of a "cone of integration." There are at least three reasons for concluding that this region of the refractivity spectrum can be safely ignored. In the first place, in practical experiments, finite antenna aperture provides a physical "cone of integration." Narrow beamwidths are not required; tens of degrees suffice (equivalent to an aperture of a few wavelengths). Secondly, in the case of a spherical wave the divergence of the wavefront reduces the effect of wide-angle scattering both through an effective increase in the scatter angle, and through increased attenuation of waves scattered at large angles (since the scattered waves are themselves spherical waves, and hence undergo 1/r decay, unlike infinite plane waves). Finally, in the case of the plane wave, solutions can be obtained for the scattering in the region of the spectrum, including the effects of depolarization (Lee and Harp, 1969, and Strohbehn and Clifford). These solutions show that, provided the propagation path is reasonably lossy (this condition is met at all wavelengths from the microwave to the optical regions), contributions from this portion of the refractivity spectrum will be negligible.

A final point concerns an assumption implicit in Sections 2 and 3—that Fourier components along the axis of the path (as opposed to transverse components making up the slab) have no effect upon the wave. This is clearly the case as far as the amplitude of the wave is concerned; a wave propagating through a uniform slab emerges with its wavefront unperturbed. However, the wavefront will suffer delay (or advancement) in phase. If the period of the Fourier component (or series of slabs, alternately retarding and advancing the wave) is small compared with the path length, the net phase perturbation will be near zero (it is at most that caused by a half-cycle of the Fourier component). If on the other hand the period is comparable to or greater than the path length, and the amplitude of the Fourier component is large enough, significant phase changes can occur. Such phase changes will affect all points in the plane of the receiver, and can be thought of as changes in the average refractive index of the atmosphere in the vicinity of the path. As such, they can be excluded from analysis concerned with scattering, and included simply as a slowly changing correction to phase-path, resulting from air-mass changes, etc.

5. PROPAGATION IN ANISOTROPIC MEDIA

In the preceding sections it has been assumed that the refractivity spectrum $\Phi(u)$ was independent of ϕ, the angle between $\bar{u}$ (the Fourier component of the refractivity field in a slab perpendicular to the path) and the plane containing the transmitter and the two receiving points. This assumption—that $\Phi(u)$ is isotropic—is not strictly valid in the atmosphere, particularly for small values of u. In this section we will consider two approaches to the treatment of anisotropic refractivity spectra $\Phi(u,\phi)$.

In the simplest case, $\Phi(u,\phi)$ is a separable function of the two variables u and ϕ:

$$\Phi(u,\phi) = f(\phi)\,\Phi'(u) \tag{5.1}$$

In this case the spectral shape of $\Phi(u,\phi)$ is constant for all values of ϕ, and only the overall magnitude changes with angle. The function $f(\phi)$ may be resolved into its Fourier components in harmonics of 2ϕ over the range $0 < \phi < \pi$, giving the general form for the spectrum

$$\Phi(u,\phi) = \Phi(u)\{1 + a_1\cos(2\phi+2b_1) + a_2\cos(4\phi+4b_2) \ldots + a_n\cos(2n\phi+2nb_n)\} \tag{5.2}$$

where a_n are the Fourier coefficients of $f(\phi)$ and b_n are the phases of the components (the angles between the axes of the components and the plane containing the transmitter and the receiving points). The Fourier coefficient a_o is absorbed into the spectrum $\Phi(u)$.

Taking the case of elliptical anisotropy ($a_n, b_n = 0$ for $n > 1$) and performing the integration of (2.14)

$$\int_0^{\pi} \Phi(u,\phi)\cos(du\cos\phi)\,d\phi \tag{5.3}$$

$$= \Phi(u)\int_0^{\pi}\{1 + a_1\cos(2\phi+2b_1)\}\cos(du\cos\phi)\,d\phi$$

$$= \Phi(u)\int_0^{\pi}\cos(du\cos\phi)\,d\phi + a_1\Phi(u)\int_0^{\pi}(\cos2\phi\cos2b_1 - \sin2\phi\sin2b_1)\cos(du\cos\phi)\,d\phi$$

The integral of the term involving $\sin2\phi$ being zero, we are left with

$$\pi\,\Phi(u)\{Jo(du) + a_1\cos(2b_1 J_2(du)\} \tag{5.4}$$

The n^{th} term in the case of general anisotropy gives rise to a similar term, of the form

$$\pi\,\Phi(u)\,a_n\cos(2nb_n)\,J_{2n}(du) \tag{5.5}$$

and the general result for amplitude covariance is:

$$C_a(d) = 4\pi^2k^2\int_0^k du\int_0^L ds\,u\Phi(u)\{Jo(du) = a_1\cos(2b_1)J_2(du) + \ldots$$

$$+ a_n\cos(2nb_n)J_{2n}(du)\}\sin^2[u^2s/2k] \tag{5.6}$$

The form of this result is applicable to phase covariance, the spherical-wave case, and higher-order functions. (5.6) has been evaluated for elliptical anisotropy in the spherical-wave geometry, and the results are shown in Figure 5.1. The parameters used were: path length L = 28 km, wavenumber k = 716 (35 GHz). The spatial covariance function is plotted for $a_1 = 0$ (central curve; isotropic case), $a_1 = 1$ with $b_1 = 0$ (upper curve), and

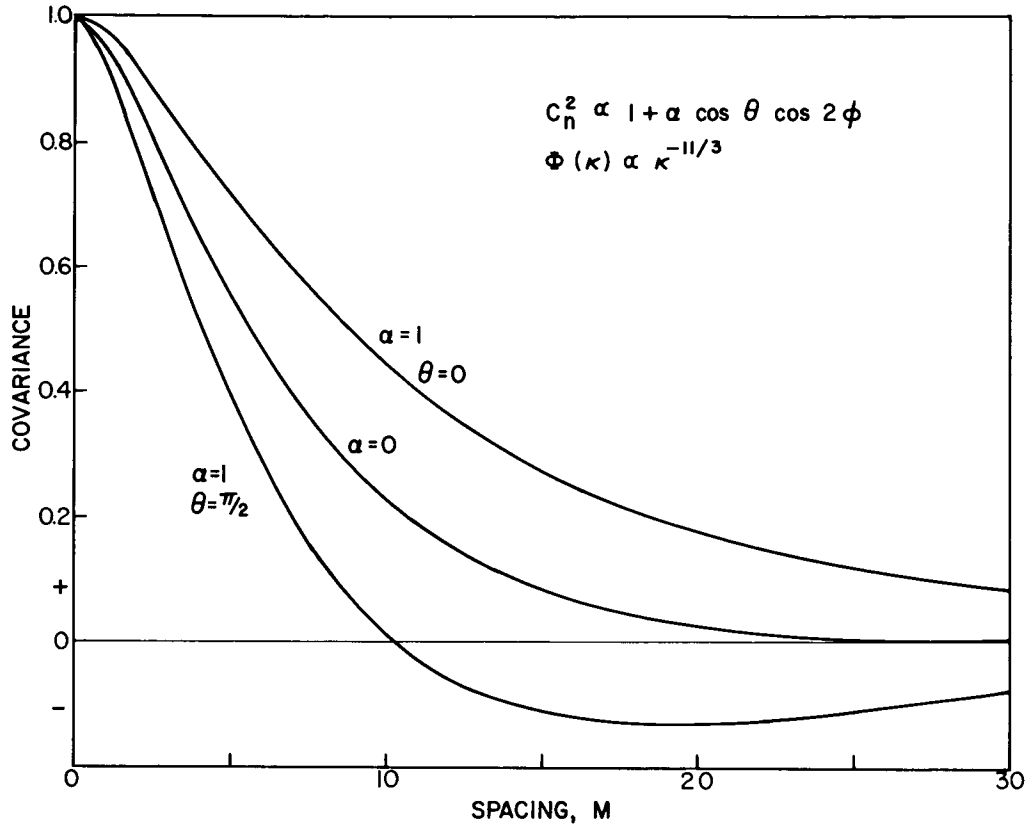

Figure 5.1. Amplitude covariance functions for three anisotropic spectra.

and $a_1 = 1$, $b_1 = \pi/2$. In an experimental situation the two curves for $a_1 = 1$ correspond to aligning the separation between the receivers parallel to and perpendicular to the major axis of the anisotropy. The resulting changes in covariance are quite marked, and affect the basic shape of the function as well as the magnitude. Note that the two curves for the anisotropic case are symmetrically displaced from the isotropic curve.

A second approach to anisotropy is to consider $\Phi(u,\phi)$ to be composed of two orthogonal components, each of which is separable in u and ϕ:

$$\Phi(u,\phi) = \Phi_h(u) \sin^2(\phi + b) + \Phi_v(u) \cos^2(\phi + b) \tag{5.7}$$

$\Phi_h(u)$ and $\Phi_v(u)$ might be the spectrum as measured in the atmosphere in the horizontal and vertical planes, and b the angle between $\bar{u}$ and the plane containing the transmitter and receiving points. This relationship is quite appropriate to the situation in the free atmosphere, where in general there are only three unique axes, defined by the vertical, the horizontal and the direction of the wind. Note that only two degrees of freedom are necessary for the calculations here, since longitudinal components of the refractivity field are assumed to have negligible effect. Expanding (5.7):

$$\Phi(u,\phi) = \Phi_h(u)(\sin^2\phi\cos^2 b + \cos^2\phi\sin^2 b + \frac{1}{2}\sin 2\phi \sin 2b \tag{5.8}$$

$$+ \Phi_v(u)(\cos^2\phi\cos^2 b + \sin^2\phi\sin^2 b - \frac{1}{2}\sin 2\phi \sin 2b$$

Performing the integrations as in (5.3):

$$\int_0^{\pi} \sin^2\phi \cos\,(d\,u\cos\phi)d\phi = \frac{\pi}{2}\,[Jo(du) + J_2(du)] \tag{5.9}$$

$$\int_0^{\pi} \cos^2\phi \cos\,(d\,u\cos\phi)d\phi = \frac{\pi}{2}\,[Jo(du) - J_2(du)] \tag{5.10}$$

As before, the terms involving $\sin 2\phi$ do not contribute to the integral. Using (5.9) and (5.10) in conjunction with (5.8):

$$\begin{aligned}\int_0^{\pi} \Phi(u,\phi)\cos\,(du\cos\phi)\,d\phi &= \\ &\frac{\pi}{2}\,[Jo(du) + J_2(du)]\,[\cos^2 b\Phi_h(u) + \sin^2 b\Phi_v(u)] \\ &+ \frac{\pi}{2}\,[Jo(du) - J_2(du)]\,[\sin^2 b\Phi_h(u) + \cos^2 b\Phi_v(U)] \\ &= \frac{\pi}{2}\,Jo(du)\,[\Phi_h(u) + \Phi_v(u)] + \frac{\pi}{2}J_2(du)\cos(2b)\,[\Phi_h(u) - \Phi_v(U)]\end{aligned} \tag{5.11}$$

The amplitude covariance (plane-wave) becomes:

$$C_a(d) = 2\pi^2 k^2 \int_0^{k} du \int_0^{L} ds\; u\{Jo(du)(\Phi_h + \Phi_v) + J_2(du)\cos(2b)(\Phi_h - \Phi_v)\sin^2[u^2 s/2k]\} \tag{5.12}$$

The same remarks as to generality apply here as to (5.6). If the spectra Φ_h and Φ_v differ only by a multiplicative constant, (5.12) reduces to (5.6), with $\Phi(u) = \Phi_h + \Phi_v$ and $a_1 = \Phi_h - \Phi_v/\Phi_h + \Phi_v$. Both Φ_h and Φ_v of (5.7) can be anisotropic spectra in the sense of (5.2). Integration over ϕ is still straightforward, the result being quite general. The spectrum can then be elliptically anisotropic as far as changes in the behavior of $\Phi(u,\phi)$ in u with ϕ are concerned, and arbitrarily anisotropic in ϕ for each of the components. Completely general anisotropy can be treated by allowing the coefficients a_n and b_n in (5.6) to functions of u.

6. TIME-LAGGED FUNCTIONS

Temporal variation of the field at a point in the receiving plane is the result of two distinct processes. The dielectric field over the region between the transmitter(s) and receivers is changing with time through various mechanisms—advection, convection, turbulent motions, and so on—resulting in corresponding changes in the field. Such changes take place on the time scale of the meteorological processes involved, typically from seconds (turbulent motions) to very large time scales (air mass changes). It is reasonable to expect that the fine scale structure of the dielectric field is more susceptible to rapid variation than large-scale structure. Such changes in the dielectric

field (and the resulting changes in received field) are in general anisotropic, inhomogeneous and non-stationary, and are therefore very difficult to treat both experimentally and theoretically.

The second process resulting in temporal variations of the dielectric field is simply motion of the atmosphere itself, either real (wind) or apparent (as due to the motion of a source). If, to take an example, the atmosphere between a transmitter and a receiver was unchanging except for a simple translation in a direction perpendicular to the transmission path, then the field at the receiver would change in exactly the same manner as if the receiver and transmitter had themselves translated, the atmosphere remaining stationary. This transformation of spatial functions to temporal functions, or Taylor's hypothesis (Taylor, (1938)), is quite convenient from both a theoretical and experimental point of view. It allows (approximately) the equivalent of measurements at many points in space to be made (expensive to do directly), simply by observing the time behavior of a quantity, providing that the velocity of the atmosphere is known.

In general, however, wind velocity in the atmosphere is not sufficiently uniform over the experimental path for a simple "frozen atmosphere" approach to yield accurate results. The next higher approximation is to consider the velocity to be a known function over the path, if this is possible in the appropriate theory.

Approaches based upon Taylor's hypothesis are approximations in two senses. First, wind velocity is assumed to be uniform at all points in a plane transverse to the path—a relatively safe assumption, since only a limited region surrounding the axis of the path itself is important. In addition, temporal variations arising from causes other than wind are neglected. The validity of this assumption depends upon the particular measurement being made. In general, measurements are sensitive only to a limited region of the spectrum of refractivity fluctuations (see Section 10), and as a result temporal variations caused by a given windspeed will lie in a given frequency range. Whether Taylor's hypothesis is appropriate will then depend upon whether significant changes occur in the appropriate region of the spectrum of refractivity fluctuations, in a time scale similar to that expected for changes due to wind. It is sufficient to note there that this condition is often satisfied to the extent that useful measurements can be made.

The extension of the theoretical development of Sections 2 through 5 to include temporal functions involving windspeed is quite straightforward. In (2.14) the quantity d represents the spatial separation of the paths to the two receivers (in this case the source is at infinity, and d is independent of path position). Since time-lagged covariance is by definition the covariance of the fluctuations at one point with the fluctuations at another point at a different time, the quantity d can be identified as the apparent spatial separation between the two paths, including both the physical separation and the apparent separation caused by drift with the wind of one of the points. That is, $d = d_o + V(s)t$, where $V(s)$ is the velocity at position s in the path, and t is the time-lag for which covariance is to be obtained. This substitution is quite general, and may be applied wherever d appears (usually in the argument of a Bessel function). For instance, in the spherical-wave case, a typical argument is (cf. (3.13)):

$$Jo\left[u \left(\frac{ds}{L} + V(s)t \right) \right] \qquad (6.1)$$

Note that V(s) is the component of the wind velocity transverse to the transmission path, the effects of longitudinal winds being quite small. In the case where $\bar{d}$ and $\overline{V(s)}$ are not parallel, the appropriate vector addition is necessary.

As an example, a family of theoretical time-lagged amplitude covariance functions is shown in Figure 6.1. The curves were calculated from the results of Section 3 (cf. (3.13)), using for $\Phi(u)$ the Kolmogorov spectrum $\Phi(u) \propto u^{-11/3}$. Path length is 28 km, k = 716, and V(s) = 5 m/s. Covariance functions are shown for 8 values of d from 0 (highest curve) to 24 m. The variation of covariance with separation d at t = 0 follows the curve in Figure 3.1 for the diverging-path geometry (with n = 11). In addition, the peaks of the covariance functions in Figure 6.1 follow the curve in Figure 3.1 for the crossed-path geometry, for separations half as great. That is, maximum time-lagged covariance is obtained when the uniform drift due to the wind has effectively moved one of the transmission paths across the other, such that they cross in the center. In this situation, the separation at the ends of the path is half the separation at t = 0. Figure 6.2 shows a typical family of curves identical in formal and path geometry to that of 6.1, but experimentally obtained rather than theoretical.

The peak-covariances of many families of the type shown in Figure 6.2 were measured over a two day period, on the path already described. The results are shown in Figure 6.3, plotted together with three theoretical curves of the type shown in Figure 3.1 (crossed-path geometry). The figures on the three curves represent the exponent of the refractivity spectrum assumed. The mean data points agree well with the theoretical curves, but individual data points differ greatly, as can be seen from the 10th and 90th percentiles. This is perhaps reasonable, for while the average wind velocity may be uniform along the path, the wind at any time may be highly non-uniform. As will be seen from the theoretical examples to follow, the first effect of a linear variation of

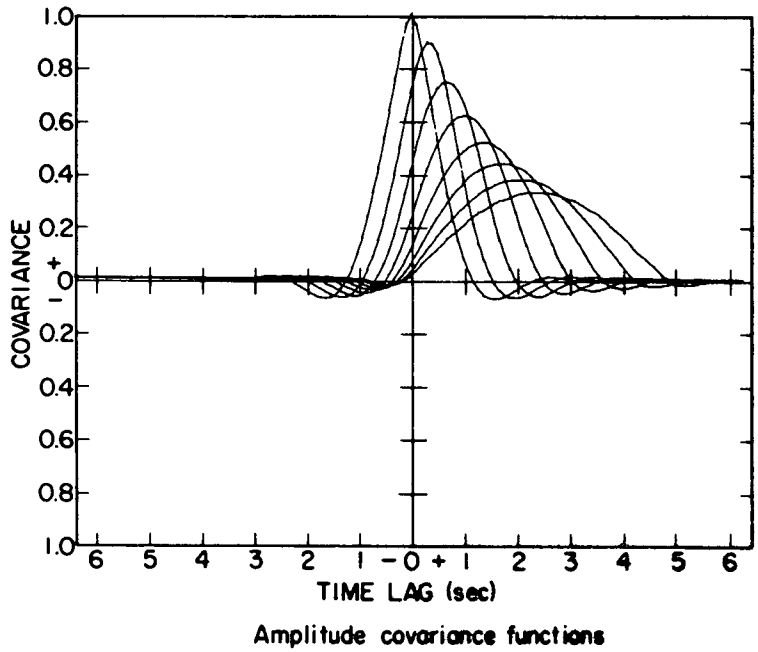

Figure 6.1. Covariance vs. time lag for uniform wind field.

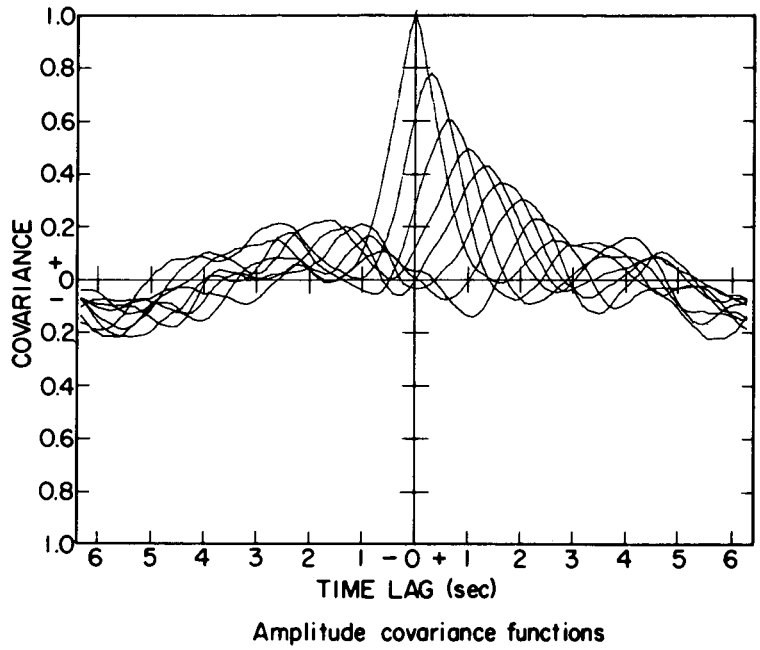

Figure 6.2. Measured covariance functions.

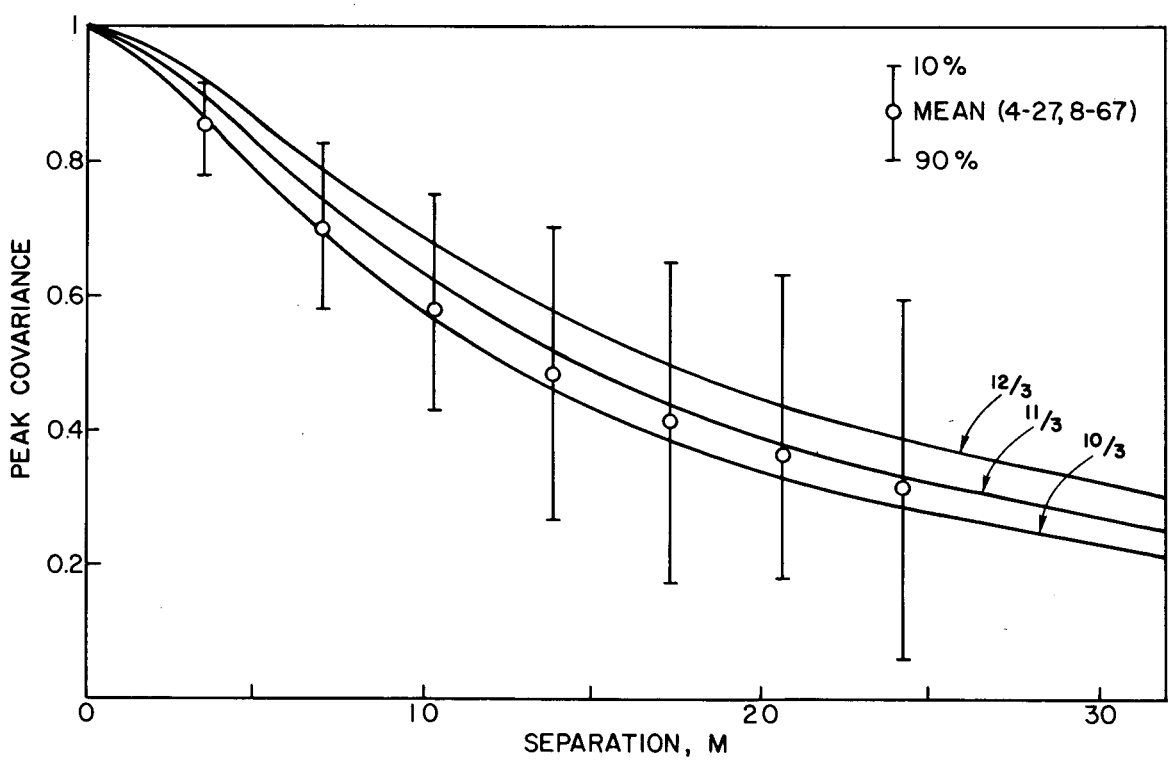

Figure 6.3. Peak time-lagged covariance vs. receiver separation, theoretical and experimental.

wind velocity along the path is to increase or decrease the peak covariances, depending upon whether the variation tends to rotate the air mass about the transmitter, or receiver, respectively.

In general the wind velocity is not uniform along the path, and in addition the refractivity spectrum may also vary along the path. As an example, Figure 6.4 shows another family of experimentally-obtained covariance functions, taken when the path was far from uniform. The curves are much more complex than those of Figure 6.2, and in fact exhibit double-peaks.

To give an indication of the effect of non-uniform wind velocity upon amplitude covariance functions, a few specific cases for which the covariance functions have been evaluated are included here. They differ from Figure 6.1 only in that different assumptions have been made concerning the wind field.

As an example of a double-peaked family of functions, Figure 6.5 was obtained for a wind field uniform at 5 m/s over the path from the transmitter to mid-path, and 7/8 of this value for the remainder of the path. Figure 6.6 was obtained for a wind field uniform at 5 m/s over the first half of the path, as is Figure 6.5, but in this case the velocity was -5 m/s over the last half of the path; that is, the windspeed was uniform, but the direction reversed at mid-path. Contributions from the two regions of the path are clearly evident in the figure. A more subtle change in the windfield was used to obtain Figure 6.7—the windspeed increased linearly from 4 m/s at the transmitter to 6 m/s at the receiver. As a result, the covariance peak value is increased, since the wind field tended to rotate the air mass about the transmitter. If the wind field were zero at the transmitter and increased linearly with distance from it, then (in the "frozen medium" approximation) the peaks of the covariance functions would all be unity, since rotation would bring a given

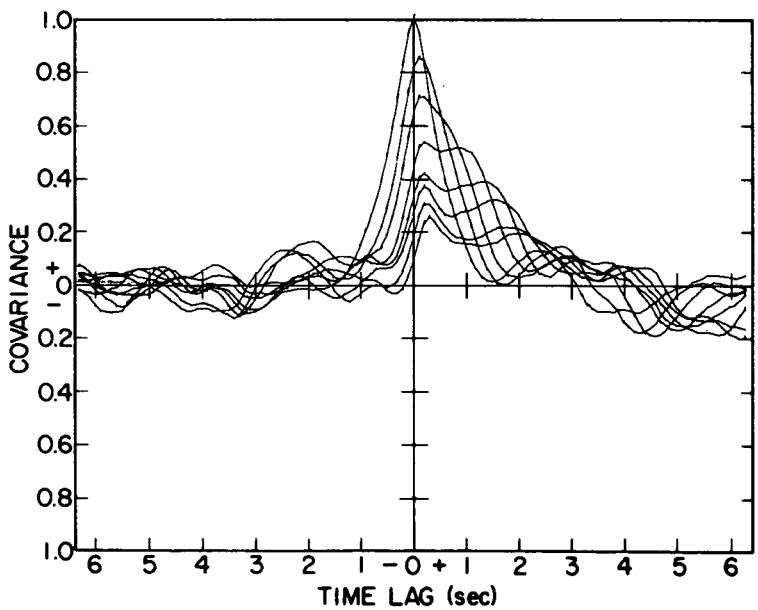

Amplitude covariance functions

Figure 6.4. Measured covariance functions for non-uniform wind field.

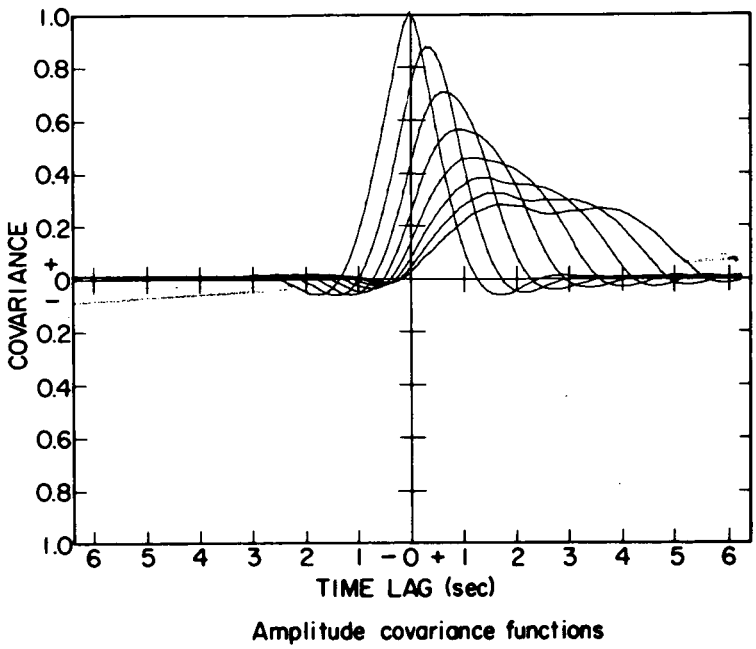

Figure 6.5. Theoretical covariance functions for bimodal wind field.

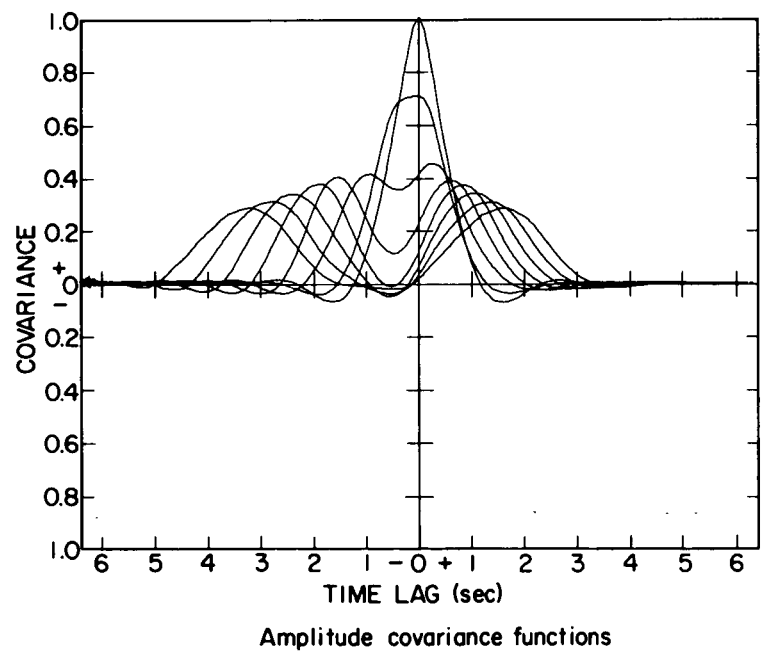

Figure 6.6. Theoretical covariance functions for wind field with direction reversal at mid-path.

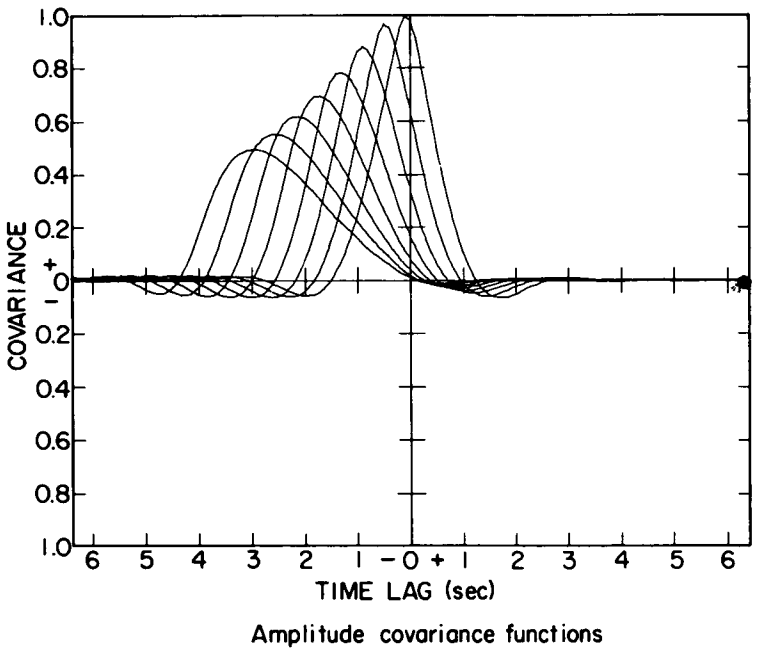

Figure 6.7. Theoretical covariance functions for wind field with uniform shear.

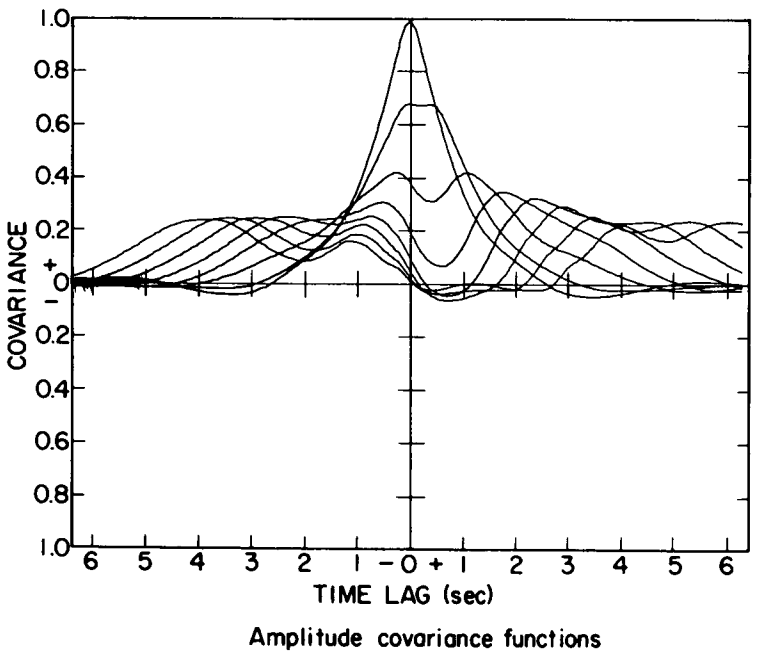

Figure 6.8. Theoretical covariance functions for wind field rotating about mid-path.

region of the atmosphere successively between the transmitter and the several receiving points. Finally, Figure 6.8 was obtained for a wind field effectively rotated around mid-path—the velocity at the transmitter was 8 m/s, decreasing linearly to zero at mid-path, and further decreasing to -8 m/s at the receiver. As can be seen from the figure, the result is quite complex.

7. HIGHER STATISTICAL FUNCTIONS

Simple covariances and structure-functions are by no means the only quantities characterizing the wave perturbations which are of interest. The number of possibilities is limitless, and this section is devoted to some important examples, which may serve as guides for generalization.

Hitherto the quantities calculated have involved the relationship between perturbations of the wave at two points in the receiving plane. A natural extension is to consider more than two points, an extension which will be seen to have considerable experimental application. Consider the covariance of difference-pairs—that is, the covariance of the difference of amplitude at two points with the difference between two other points. If the four points are co-linear, the pairs are separated by d, and members of a pair separated by e, it is easily shown that

$$C(d,e) = 2C(d) - C(d+e) - C(d-e) . \tag{7.1}$$

When applied to amplitude or phase covariance, the Bessel term of (3.18) and (3.22) becomes

$$Jo\left(\frac{dsu}{L}\right) \rightarrow 2Jo\left(\frac{dsu}{L}\right) - Jo\left(\frac{(d+e)su}{L}\right) - Jo\left(\frac{(d-e)su}{L}\right) . \tag{7.2}$$

The same result may of course be obtained directly by starting with the magnitude of the perturbation, taking differences, and proceeding as before. As an example of the utility of (7.2), combined with (3.17), several computed phase-covariance functions are shown in Figure 7.1. The upper four curves show the normal (2 point) covariance function; for all cases a Kolmogorov spectrum was assumed—the cases differ only in the value of u at which the power-law spectrum was terminated at the lower end (the "outer-scale" L_o). Such termination is of course required in order that the phase-covariance be finite. Path parameters were $L = 2.8 \times 10^4$, $k = 716$. The values chosen correspond to values of L_o from 50 to 100 m. The lower four curves represent 4-point covariance functions of the type just described. The same values of L_o were used, the relative narrowness of the function reflecting the emphasis that the differential-process places upon small-scale perturbations. The value of e used was 3.5 m. The two points on the plot represent averages of experimental data obtained on the path already described. The particular utility of such difference-pair covariances in this case is evident, since phase-difference between two points on the wavefront is much easier to measure experimentally than absolute phase.

In the event that the four points in such a measurement are not co-linear, or equally-spaced, the results may be expressed as four terms involving the four separations; an important situation involves the four points in a rectangular situation:

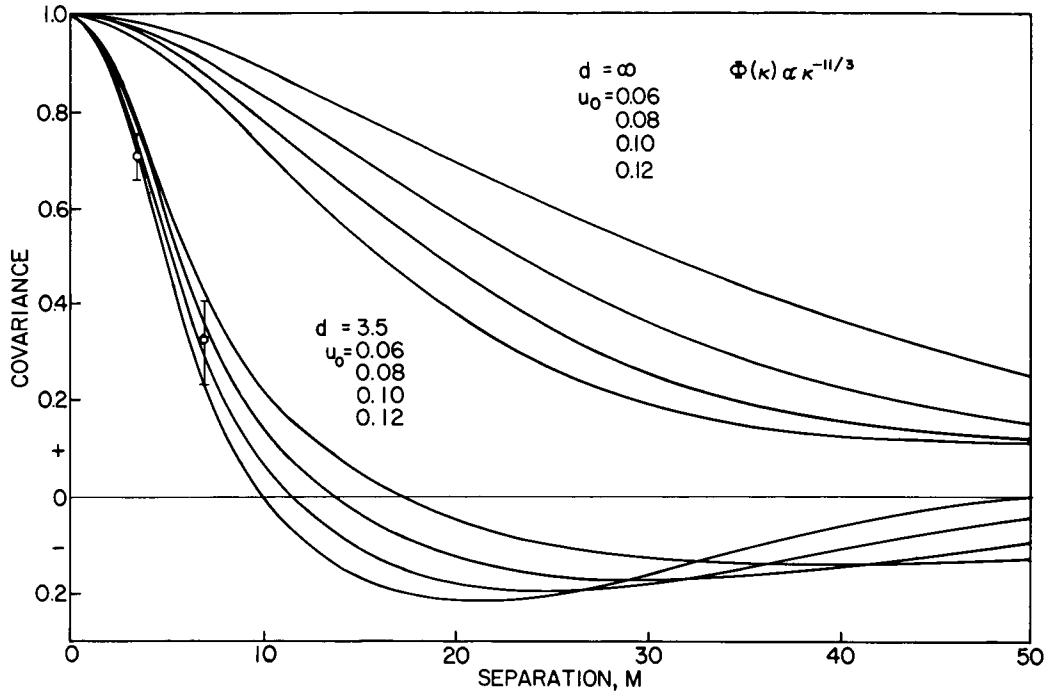

Figure 7.1. Phase and phase-difference covariance functions, for different values of the "outer scale."

$$\mathrm{Jo}\left(\frac{dsu}{L}\right) \rightarrow 2\mathrm{Jo}\left(\frac{dsu}{L}\right) - 2\mathrm{Jo}\left(\sqrt{d^e + e^2}\,\frac{su}{L}\right) \tag{7.3}$$

If the separation e in (7.2) and (7.3) is made arbitrarily small, and the resulting covariance is normalized by 1/e, the result is the covariance of the slope of the quantity. Performing this operation on (7.2), the result is

$$\frac{s^2 u^2}{2L^2}\left(\mathrm{Jo}\left(\frac{dsu}{L}\right) - J_2\left(\frac{dsu}{L}\right)\right). \tag{7.4}$$

Using (7.4) with (3.17), covariance of the slope of the phasefront is obtained; that is, covariance of that component of angle-of-arrival parallel to the separation d. When the operation is performed on (7.3), the result differs only in that the minus sign of (7.4) becomes a plus sign, and covariance of the perpendicular component of the slope is obtained.

With the exception of the wave structure-function, all quantities calculated thus far have involved either the amplitude or phase perturbations on the wavefront, but not both. This separation is somewhat artificial; mixed quantities are easily obtained. As an example, the covariance of the amplitude fluctuations at one point in the receiving plane with the phase fluctuations at another point is

$$C_{ap}(d) = 2\pi^2 k^2 \int_0^k du \int_0^L ds\, u\Phi(u)\, \mathrm{Jo}\left(\frac{dsu}{L}\right) \sin\left(\frac{u^2 s(L-s)}{kL}\right) \tag{7.5}$$

Similarly, the covariance between the amplitude at one point and the difference between the phases at two other points differs from (7.5) in that

$$\mathrm{Jo}\left(\frac{dsu}{L}\right) \rightarrow \mathrm{Jo}\left(\frac{d+\frac{e}{2}su}{L}\right) - \mathrm{Jo}\left(\frac{\left(d-\frac{e}{2}\right)su}{L}\right) \tag{7.6}$$

Where the amplitude is measured at (O), and the phase at d + e/2 and d - e/2. A plot of this function, calculated for a Kolmogorov spectrum (with e = 3.5 m, other parameters as before), is shown in Figure 7.2. An experimentally obtained function of a similar nature is shown in Figure 7.3. It shows the covariance between the amplitude and the phase difference at two points separated by 3.5 m, as a function of time-lag.

The covariance between the amplitude and angle-of-arrival may be similarly obtained. It differs from (7.5) in that

$$\mathrm{Jo}\left(\frac{dsu}{L}\right) \rightarrow \frac{us}{2L} J_1\left(\frac{dsu}{L}\right) . \tag{7.7}$$

As might be expected, this is also an odd-function.

As a final example, the amplitude covariance between waves with different wave-numbers k_1 and k_2 is

$$C_f(d) = 4\pi^2 k_1 k_2 \int_0^L ds \int_0^{\sqrt{k_1 k_2}} du\, u\Phi(u)\, \mathrm{Jo}\left(\frac{dsu}{L}\right) \sin\left(\frac{u^2 s(L-s)}{2k_1 L}\right) \cdot \sin\left(\frac{u^2 s(L-s)}{2k_2 L}\right) \tag{7.8}$$

An evaluation of this integral for a Kolmogorov spectrum is shown in Figure 7.4. Note that the covariance (for d = O) is quite high over several octaves.

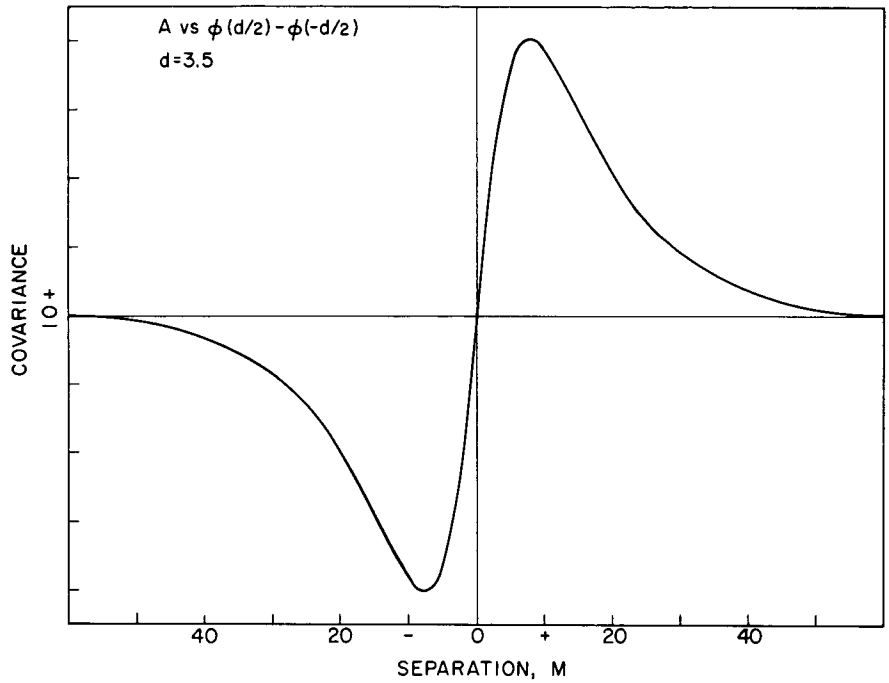

Figure 7.2. Amplitude vs. phase-difference covariance function.

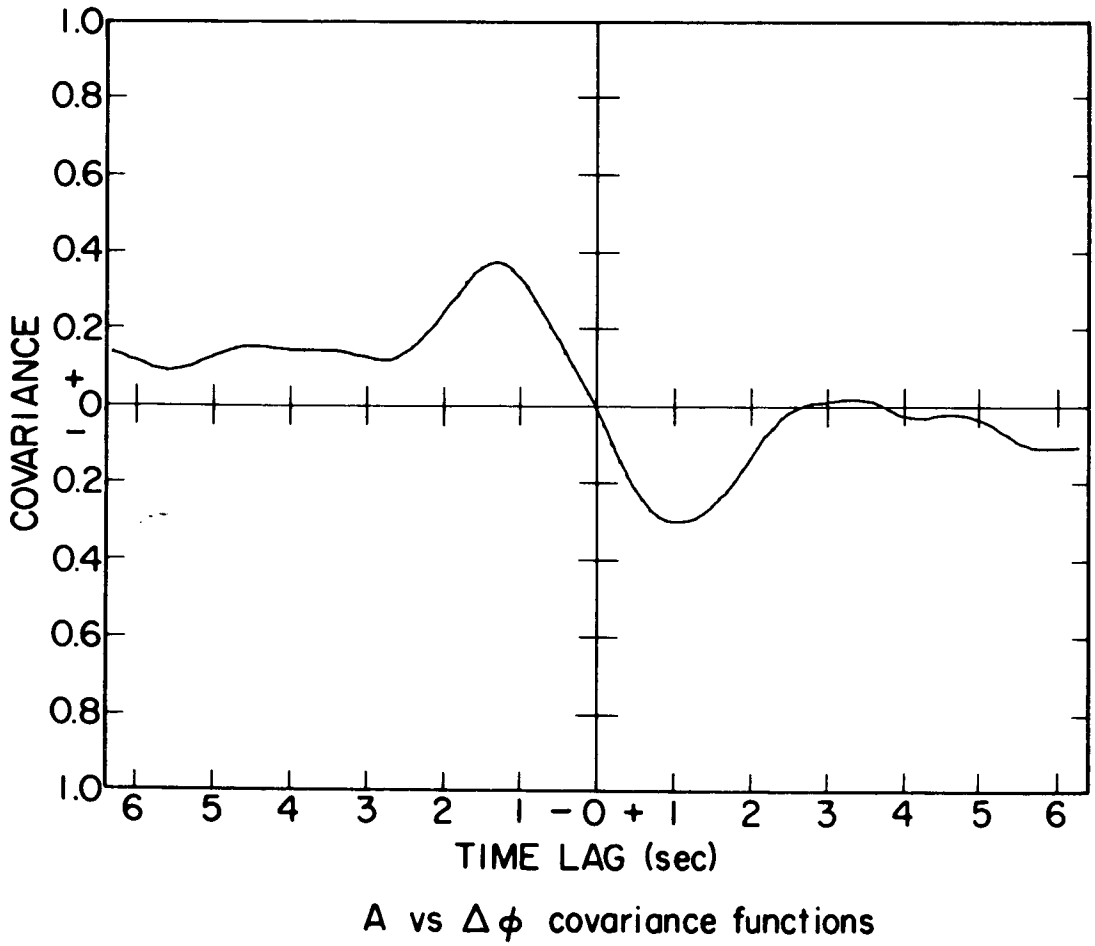

Figure 7.3. Experimental amplitude vs. phase-difference covariance function.

C.2

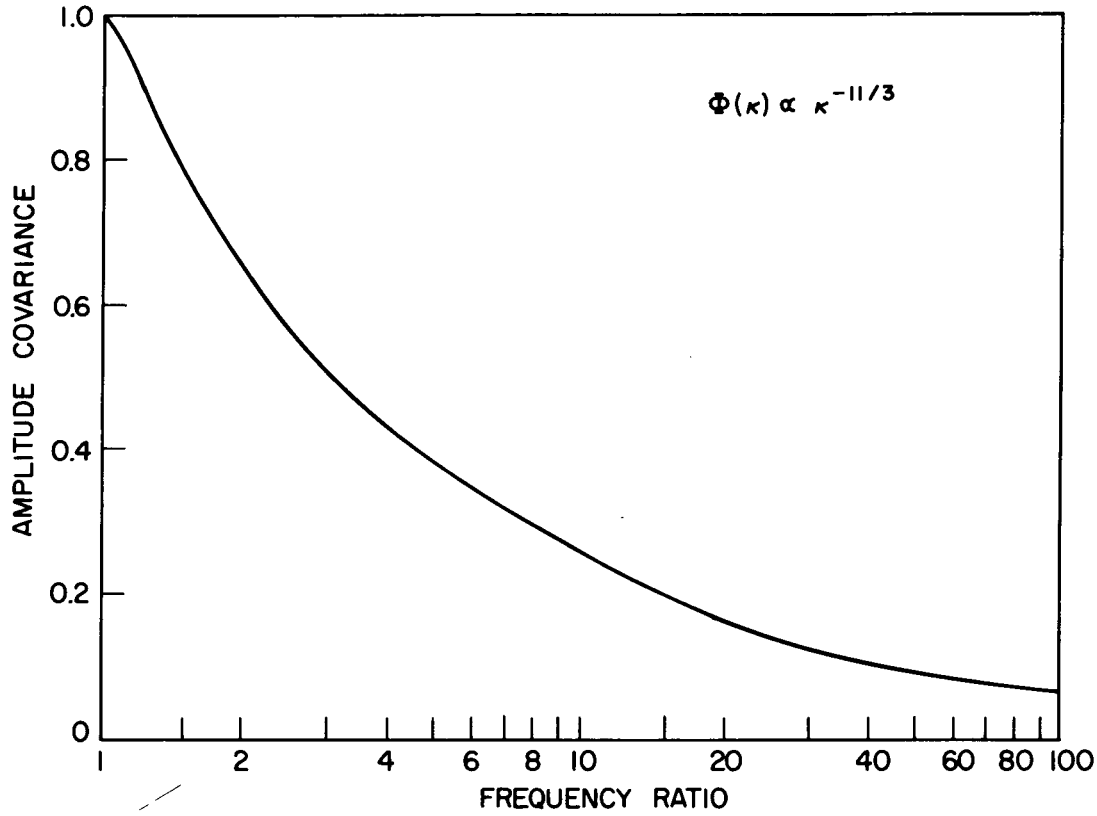

Figure 7.4. Amplitude covariance vs. frequency separation.

8. FINITE TRANSMITTING AND RECEIVING APERTURES

In the previous sections receiving apertures have been considered to be points; in the development which follows finite apertures are equated with assemblages of such points, with some weighting factor. In the geometry of the figure power is radiated from an aperture in the plane z = O, through a perturbing slab of the kind already discussed (located at z = s), to a point receiver located at (x_o, y_o, L). The weighting factor at the aperture will be taken to be Gaussian.

$$W = \frac{1}{2\pi\sigma_t^2} \exp\left[-\frac{x^2 + y^2}{2\sigma^2}\right], \tag{8.1}$$

$$\text{where } \frac{1}{\sigma^2_t} = \frac{1}{2} - \frac{ik}{F}$$

The physical size of the aperture is σ_t (the standard deviation of the Gaussian), and the focal length is F (i.e., if $F = \infty$, the phase illumination across the aperture is uniform). The differential field dE_t at P from a point at (x_t, y_t, O) on the aperture is (cf. (3.8)):

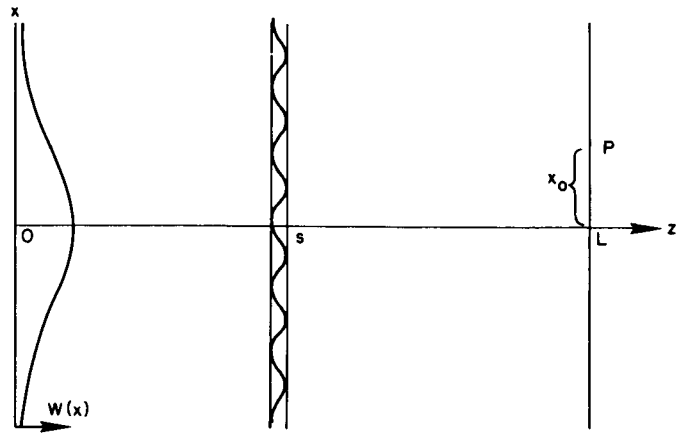

Figure 8.1.

$$dE = \frac{\exp(-ikL)}{L} \exp\left[\frac{-ik}{2L}(x_o - x_t)^2 + (y_o - y_t)^2\right] \cdot W\, dx_t dy_t \cdot \tag{8.2}$$
$$\left[1 + ika \cdot dz \cdot \exp\left(\frac{iu^2 s(L-s)}{2kL}\right) \cos\left(\frac{x_o us}{L} + \frac{x_t(L-s)}{L} + bu\right)\right].$$

As in the spherical-wave case, the perturbation at s lies along the x-axis. The total differential field dE_t at p is simply the integral of (8.2) over all points x_t and y_t on the transmitting aperture

$$dE_t = \frac{\sigma^2 \exp(-ikL)}{\sigma_t^2(L+ik\sigma^2)} \exp\left[\frac{-ik(x_o^2 + y_o^2)}{2(L + ik\sigma^2)}\right] \cdot \tag{8.3}$$
$$\left[1 + ikadz \exp\left(\frac{iu^2 s(L-s)}{2kL}\right) \exp\left(\frac{-u^2(L-s)^2\sigma^2}{2L(L+ik\sigma^2)}\right) \cos\left(x_o u \frac{s+ik\sigma^2}{L+ik\sigma^2} + bu\right)\right].$$

Since a is a small quantity, terms in a^2 can be neglected, and the field perturbation at P is (cf. (2.7)),

$$dP_a = \mathcal{R}\left[ikadz \exp\left(\frac{iu^2 s(L-s)}{2kL}\right) \exp\left(\frac{-u^2(L-s)^2\sigma^2}{2L(L+ik\sigma^2)}\right) \cos\left(ux_o \frac{s+ik\sigma^2}{L+ik\sigma^2} + bu\right)\right]. \tag{8.4}$$

The phase perturbation is of course the imaginary part of the quantity in (8.4). The amplitude covariance is obtained by summing the products of the perturbations at two points. Choosing one point at (x_o, y_o, L) and the other at (O, O, L), and proceeding as in (3.11),

$$dC_a(x_o) = \frac{1}{2}\mathcal{R}\{k^2 \int_0^L i \cdot \exp\frac{(iu^2 s_1(L-s_1))}{2kL} \exp\frac{(-u^2(L-s_1)^2\sigma^2)}{2L(L+ik\sigma^2)} \cdot$$

$$\int_0^L i \cdot \exp\frac{(iu^2 s_2(L-s_2)}{2kL} \exp\frac{-u^2(L-s)_2^2\sigma^2}{2L(L+ik\sigma^2)}$$

$$\langle a(u,s_1)\cos\left(ux_1\frac{s_1+ik\sigma^2}{L+ik\sigma^2}+b_1u\right)\cdot a(u,s_2)\cos\left(ux_2\frac{s_2+ik\sigma^2}{L+ik\sigma^2}+b_2u\right)\rangle\, ds_1 ds_2$$

$$+k^2\int_0^L (s_1 \text{ terms})\int_0^L (s_2 \text{ terms})^*$$

$$\langle a(u,s_1)\cos(\ldots+b_1u)\quad a^*(u,s_2)\cos(b_2u)\rangle\, ds_1 ds_2\,\}, \tag{8.5}$$

where * denotes the complex conjugate. In expression (8.5) we have used the relation:

$$\mathcal{R}(A)\cdot\mathcal{R}(B) = \frac{1}{2}\mathcal{R}[A(B+B^*)], \tag{8.6}$$

where A and B are complex quantities.

As in the spherical-wave case, we may perform the cross product integration in (8.5) under the conditions, $k \gg u$ and $L \gg \lambda$, with the result:

$$dC_a(x_o) = 2\pi^2\mathcal{R}\{\int_0^L u\Phi(u)\left[\exp\left(\frac{iu^2 s(L-s)}{2kL}\right)\exp\left(\frac{-u^2(L-s)^2\sigma^2}{2L(L+ik\sigma^2)}\right)\right]\cdot$$

$$([\ldots]-[*])\cos\left(ux_o\frac{s+ik\sigma^2}{L+ik\sigma^2}\right)ds\,\}, \tag{8.7}$$

where [*] denotes the complex conjugate of the previous quantity in similar brackets.

The total covariance is the integral of (8.7) over all wavenumbers $\bar{u}$. Proceeding as in the sperical-wave case (cf. (3.13)), where $d\bar{u} = u\,du\,d\phi$, and recognizing the x-coordinate separation of the receiving points (x_o), as $d\cos(\phi)$,

$$C_a(d) = 2\pi^2k^2\mathcal{R}\int_0^k du\int_0^L ds\, u\Phi(u)\,Jo\left(\frac{du(s+ik\sigma^2)}{L+ik\sigma^2}\right)\exp(Q)\,(\exp(Q^*)-\exp(Q)) \tag{8.8}$$

$$\text{where } Q = \left(\frac{-u^2(L-s)(s+ik\sigma^2)}{2ik(L+ik\sigma^2)}\right).$$

Phase-covariance is obtained similarly.

$$C_p(d) = 2\pi^2 k^2 \mathcal{R} \int_0^k du \int_0^L ds\, u\Phi(u)\, Jo\left(\frac{du(s+ik\sigma^2)}{L+ik\sigma^2}\right) \exp(Q)\,(\exp(Q^*)+\exp(Q)) \tag{8.9}$$

These results are essentially identical to those of Schmeltzer (1967). They differ only in the assumption of exp (-ikr) for the form of a propagating wave, rather than exp (+ikr), with the result that the solutions are conjugate to those of Schmeltzer.

If σ^2 is real—that is, if the transmitting aperture is focused at infinity—(8.8) and (8.9) may be written

$$c_{ap}(d) = 2\pi^2 k^2 \mathcal{R} \int_0^k du \int_0^L ds\, u\Phi(u)\, Jo\left(\frac{du(s+ik\sigma^2)}{L+ik\sigma^2}\right) \exp\left(\frac{-u^2(L-s)^2\sigma^2}{L^2+k^2\sigma^4}\right) \cdot$$

$$\left[1 \mp \exp\left(\frac{iu^2(L-s)(sL+k^2\sigma^4)}{k(L^2+k^2\sigma^4)}\right)\right] . \tag{8.10}$$

A logical extension of these results is to consider the receiving as well as the transmitting apertures to be finite. The result of similar development for Gaussian receiving and transmitting apertures is

$$C_{ap}(d) = 2\pi^2 k^2 \mathcal{R} \int_0^L du \int_0^k ds\, u\Phi(u)\, Jo\left(\frac{du(s+ik\sigma_t^2)}{L+ik(\sigma_t^2+\sigma_r^2)}\right) (RR^* \mp RR) ,$$

$$R = \exp\left(\frac{iu^2 s(L-s)}{2kL}\right) \exp\left[\frac{iu^2}{2L}\left(\frac{(L-s)^2\sigma_t^2}{L+ik\sigma_t^2} + \frac{L\sigma_r^2(s+ik\sigma_t^2)^2}{(L+ik\sigma_t^2)(L+ik(\sigma_t^2+\sigma_r^2))}\right)\right] \tag{8.11}$$

where σ_t and σ_r refer to the transmitting and receiving apertures.

The plane-wave situation can be obtained from (8.11) by allowing σ_t to approach infinity, σ_t being real:

$$C_{ap}(d) = 2\pi^2 k^2 \int_0^k du \int_0^L ds\, u\Phi(u)\, Jo(du) \exp(-u^2\sigma_r^2)\left[1 \mp \cos\left(\frac{u^2(L-s)}{k}\right)\right] \tag{8.12}$$

This expression differs from the plane-wave, point-receiving-aperture result by the term $\exp(-u^2\sigma_r^2)$, which has the effect of reducing contributions from high wavenumbers u.

If the transmitting aperture is not infinite, but the receiver is nevertheless well within the near-field of the transmitter aperture (a common situation in optical experiments), then $k\sigma_t^2 \gg L$, and (8.11) may be approximated (σ_t^2 real).

$$C_{a_p}(d) = 2\pi^2 k^2 \int_0^k du \int_0^L ds\, u\Phi(u)\, Jo\left[\frac{du\sigma_t^2}{\sigma_t^2+\sigma_r^2}\right] \exp\left[\frac{-u^2\sigma_t^2\sigma_r^2}{\sigma_t^2+\sigma_r^2}\right] \cdot$$

$$\left[1 \mp \cos\left(\frac{u^2(L-s)}{k}\right)\right] . \tag{8.13}$$

In obtaining (8.5) it was assumed that one of the receiving points lay on the z-axis; if this is not the case, (8.5) may be rewritten

$$dC_a(x_1-x_2) = \frac{1}{2}\mathcal{R}\{k^2 \int_0^L i.\exp\left(\frac{iu^2 s_1(L-s_1)}{2kL}\right) \exp\left(\frac{-u^2(L-s_1)^2\sigma^2}{2L(L+ik\sigma^2)}\right) \cdot$$

$$\int_0^L (s_2 \text{ terms}) \cdot \langle a(u,s_1) \cos\left(ux_1 \frac{s_1+ik\sigma^2}{L+ik\sigma^2} + b_1 u\right) \cdot$$

$$a(u,s_2) \cos\left(\left(x_2, s_2 \text{ terms}\right) + b_2 u\right) \rangle\, ds_1 ds_2$$

$$+ k^2 \int_0^L (s_1 \text{ terms} \cdot \int_0^L (s_2 \text{ terms}) \cdot$$

$$\langle a(u,s_1) \cos(\ldots) \cdot a^*(u,s_2) \cos(*)\rangle\, ds_1 ds_2 \} . \tag{8.14}$$

As before, we may reduce this integral under the one additional assumption $x_1, x_2 \ll L$ (cf. (8.7)).

If $\bar{d}_1$ and $\bar{d}_2$ are the vectors from (O,O,L) to the two receiving points, and ϕ and $(\phi + \theta)$ are the angles between these vectors and the axis of the perturbation, then,

$$x_1 = |\bar{d}_1| \cos(\phi), \tag{8.15}$$

$$x_2 = |\bar{d}_2| \cos(\phi + \theta) .$$

Expressing the total covariance C(d) as the integral of (8.14) over all $\bar{u}$, and performing the ϕ integration (cf. (8.8)):

$$C_{a_p}(d) = 2\pi^2 k^2 \mathcal{R} \int_0^k du \int_0^L ds\, u\Phi(u) \left(|\exp Q|^2 J_o\left[u|\bar{d}_1 R - \bar{d}_2 R^*|\right] \mp (\exp Q)^2 J_o \right.$$

$$\left. \left[uR|\bar{d}_1 - \bar{d}_2|\right]\right) , \tag{8.16}$$

$$\text{where } R = \frac{s+ik\sigma^2}{L+ik\sigma^2} \text{ and } Q = \frac{-u^2(L-s)}{2ik} R$$

This result is essentially that of Ishimaru (1968). It may be extended to include finite receiving as well as transmitting apertures:

$$C_{\substack{a\\p}}(d) = 2\pi^2 k^2 \mathcal{R} \int_0^k du \int_0^L ds\, u\Phi(u) \left(|P|^2 J_o \left[u|\bar{d}_1 S - \bar{d}_2 S^*| \right] \mp P^2 J_o \left[uS|\bar{d}_1 - \bar{d}_2| \right] \right) \tag{8.17}$$

where

$$P = \exp\left(\frac{iu^2 s(L-s)}{2kL} \right) \exp\left[\frac{u^2}{2L} \left(\frac{(L-s)^2 \sigma_t^2}{L + ik\sigma_t^2} + \frac{L\sigma_r^2 (s+ik\sigma_t^2)^2}{(L+ik\sigma_t^2)(L+ik(\sigma_t^2+\sigma_r^2))} \right) \right]$$

$$S = \frac{s+ik\sigma_t^2}{L+ik(\sigma_t^2+\sigma_r^2)}$$

The development of expressions for anisotropic spectra $\Phi(u)$ of Section 5 may be applied readily to the finite aperture treatment of this section. The anisotropic spectrum (5.7) can be included in the ϕ-integration preceding (8.5) or (8.16), with results of the form of (5.12) obtaining.

9. PROPAGATION IN A RANDOM LOSSY MEDIUM

Thus far the propagation medium has been considered to be transparent—that is, the refractive index has been assumed to be real. Strictly speaking this is not the case in the atmosphere, although it is a good approximation in the microwave and optical portions of the spectrum. For other regions of the spectrum, particularly the millimeter-wave and infrared regions, moderate to very severe attenuation occurs, primarily resulting from molecular absorption lines (especially those of the water molecule).

Extension of the techniques used in Sections 2 and 3 to a medium with a complex refractive index is straightforward, and indeed the results may be simply guessed at the start. Considering a single Fourier component of the refractivity field as acting as a diffraction grating, we have noted that an additional pair of waves is generated by the grating, and that these waves lag the original wave by 90° at the grating. The sum of the three waves varies in amplitude as the sine of a function depending upon the distance from the grating (2.7). If the refractive perturbation a (cf. (2.3)) is now made complex, an additional pair of waves is created, propagating at the same angles as those caused by the real portion of the refractive index, but in phase with the original wave at the grating. Since these waves lack the 90° phase shift at the grating, their sum with the original wave is a cosine function of the distance from the grating. Note that this cosine relationship is that appropriate for the phase fluctuations due to the real part of the refractive index. In the final result, the relationships between amplitude and phase perturbations resulting from the imaginary portion of the refractive index, are identical to those for the phase and amplitude, respectively, resulting from the real part; that is, the role of a given scatterer is reversed in the two cases.

Derivation of results for the spherical-wave geometry follows. Naturally the same approach is valid for the plane-wave situation. From (3.8),

$$dE_t = 1 - ika\, dz \exp\left(\frac{iu^2 s(L-s)}{2kL}\right) \cos\left[u\left(\frac{xs}{L} + b\right)\right] \tag{9.1}$$

If a (the magnitude of the phase perturbation) is complex,

$$a = \sqrt{\Phi_r(u)} + \sqrt{\Phi_i(u)} = R + iI \tag{9.2}$$

and c is the correlation coefficient between the real and imaginary parts of a, then the perturbation of amplitude in the plane z = L is

$$dP_a = ka\, dz \cos\left(u\left(\frac{xs}{L} + b\right)\right)\left[R\sin\frac{u^2 s(L-s)}{2kL} + I\cos\frac{u^2 s(L-s)}{2kL}\right] \tag{9.3}$$

Performing the cross-product integration of (3.11),

$$dC_a(x_1 - x_2) = 4\pi k^2 \int_0^L ds \cos\left(\frac{su}{L}(s_1 - x_2)\right) \cdot \left[R^2 \sin^2 \frac{u^2 s(L-s)}{2kL} + I^2 \cos^2 \frac{u^2 s(L-s)}{2kL} + cRI \sin \frac{u^2 s(L-s)}{2kL}\right] \tag{9.4}$$

and the total covariance is:

$$C_a(d) = 4\pi^2 k^2 \int_0^k du \int_0^L ds\, J_o \frac{dsu}{L} \cdot u \cdot \left[\Phi_r(u) \sin^2\left(\frac{u^2 s(L-s)}{2kL}\right) + \Phi_i(u) \cos^2\left(\frac{u^2 s(L-s)}{2kL}\right) + c\sqrt{\Phi_r(u)\,\Phi_i(u)} \cdot \sin\left(\frac{u^2 s(L-s)}{kL}\right)\right] \tag{9.5}$$

If the real and imaginary spectra are related by a multiplicative constant such that $\Phi_i(u) = m^2 \Phi_r(u)$, then

$$C_a(d) = 4\pi^2 k^2 \int_0^k du \int_0^L ds\, u\Phi_r(u)\, J_o\left(\frac{dsu}{L}\right) \cdot \left[\sin^2\left(\frac{u^2 s(L-s)}{2kL}\right) + m^2 \cos^2\left(\frac{u^2 s(L-s)}{2kL}\right) + cm \sin\left(\frac{u^2 s(L-s)}{kL}\right)\right]. \tag{9.6}$$

Phase covariance is obtained by simply interchanging $\sin^2()$ and $\cos^2()$ terms:

$$C_p(d) = 4\pi^2 k^2 \int_0^k du \int_0^L ds\, u\Phi_r(u)\, J_o\left(\frac{dsu}{L}\right) \cdot \left[\cos^2\left(\frac{u^2 s(L-s)}{2kL}\right) + m^2 \sin^2\left(\frac{u^2 s(L-s)}{2kL}\right) + cm \sin\left(\frac{u^2 s(L-s)}{kL}\right)\right] \tag{9.7}$$

Other quantities are similarly obtained. For example, the wave structure function:

$$D(d) = 8\pi^2 k^2 \int_0^k du \int_0^L ds\, u\Phi_r(u) \left[1-Jo\left(\frac{dsu}{L}\right)\right]\left[1+m^2+2\,cm\,\sin\left(\frac{u^2 s(L-s)}{kL}\right)\right] \tag{9.8}$$

In the likely case where either $\Phi_r(u)$ or $\Phi_i(u)$ dominates, the cross-term 2 cm · sin() will not be important (as it is oscillatory about zero in both u and s).

In order to estimate the value of m, the ratio of the magnitudes of the real and imaginary fluctuating components of the refractive index, consider the following argument:

A plane-wave propagating along the z-axis in a medium of refractive index n, exp(-iknz), where n = A + iB, experiences an excess phase-path over free-space of z(A-1), and a transmittance of exp(-kzB). If the predominant mechanism for refractivity variations is local density change (as by temperature fluctuations), then changes in excess phase path will occur in proportion to the logarithm of changes in transmittance. That is, the fluctuating component of (A-1) will be of approximately the same ratio to the average excess phase path (A_o-1), as the fluctuating component of exp(-kzB) is to the average transmittance exp(-kzB_o). Thus

$$m = \frac{B_o}{(A_o-1)} = -\frac{\log_e(\text{Transmittance})}{kL(A_o-1)} \tag{9.9}$$

At the surface of the earth $A_o - 1 = .0003$; thus

$$m = -\frac{\log_e(\text{Transmittance})}{.0003kL} = .06\,\lambda\ (\text{attenuation}) \tag{9.10}$$

where λ is the wavelength in meters, and the attenuation is measured in db/km.

It appears unlikely that m can approach unity in practical situations, for (9.10) implies that losses of 16 db/1000 wavelengths would be required. To give some more realistic examples, for $\lambda = 10^{-2}$m and a loss of 0.3 db/km, m would be about 2×10^{-4}; for $\lambda = 10^{-6}$ and a loss of 30 db/km, m would be about 2×10^{-6}. Thus, in these cases, the lossy portion of the refractive index could be safely ignored as far as the wave structure function or phase covariances are concerned.

This is not necessarily the case, however, for amplitude covariances, even with such low values of m, due to the nature of the "filter functions" present in the integral (9.6). While the contribution of the real part of the refractive index to amplitude covariance is zero at u = 0 and rises to a peak at blob sizes of about a Fresnel zone (because of the $\sin^2$ term in (9.6), the filter function for the imaginary part is quite different. In the latter case the weighting is maximum at u = 0, and is minimum at the peak of the contribution from the real part. As a result, amplitude fluctuations originating from variations of the imaginary part of the refractive index, at low values of u, are emphasized by the spectrum $\Phi(u)$, which rises steeply for low u. Thus, while m^2 may be only 10^{-6}, the spectrum may be stronger by a factor of 10^4 or more at the lower u. When such contributions to amplitude covariance are appreciable, they will tend to broaden the covariance function, as well as increase the variance. The data points in Figure 3.2, for example, may be slightly affected.

10. "FILTER FUNCTIONS" FOR VARIOUS QUANTITIES

It is instructive to consider the integrands of the expressions derived in the preceding sections as composed of three types of multiplicative terms. The first term is simply the power spectrum of the refractive irregularities, the energy input to the scattering process. This term is the only connection between the integrand and the medium—the other portions of the integrand are dependent only upon the geometry of the situation (with some exceptions to be noted presently). In this section, $\Phi(u)$ is taken to be u times the spectrum appearing in previous sections. Hence, for a Kolmogorov turbulence, this section takes $\Phi(u) = u^{-8/3}$ rather than $u^{-11/3}$.

The second term is unique in being a function of the path-separation in (for example) covariance functions. It serves to relate the perturbations present at one point in the receiving plane to those at another point, and in general goes to unity as the two points become coincident (as in the case of variance). In the expressions derived in this paper this term is always a Bessel function of the first kind. In two cases not considered in this section (time-lagged functions and anisotropic media), atmospheric parameters also enter into this term.

The third term, the subject of this section, is generally referred to as a "filter function," since it weights selectively the first term. It is a measure of the effect produced by an irregularity of a given wavenumber u, at a given position s along the path; that is, it measures the scattering efficiency of the perturber. The "filter function" is a function of the geometrical factors s,u,L (path length), k (wavenumber of the electromagnetic wave), and σ (the size of the transmitting aperture). In many of the examples to follow, the second term mentioned above will be included in the "filter function," adding the receiver separation d to the variables.

The importance of "filter functions" becomes clear when attempts are made to interpret experimental measurements in terms of atmospheric parameters. A single measurement obviously cannot uniquely determine a number of parameters, and it is necessary to determine those parameters to which the measurement is most sensitive. If the more sensitive parameters are well known, attention can be directed to less sensitive parameters; if not, unique determination of the less sensitive parameters is not possible. As an example, measured spatial amplitude-covariance functions readily yield values for a very general parameter, the slope of the refractivity spectrum. However, the appropriate "filter function" (Figure 10.17) shows that such a measurement is sensitive to only a narrow range of wavenumber u. Thus the measured spectral slope is probably only representative of that portion of the spectrum in the vicinity of the peak of the "filter function."

The remainder of this section is devoted to examples of "filter functions" of four distinct types. The first type is the simple "filter function" as defined above. It is the evaluation of the integral in question (less the refractivity spectrum $\Phi(u)$) over all variables with the exception of u, and is plotted as a function of u, for several values of the path separation d. The second type is similar to the first, but is plotted for several values of the receiving or transmitting aperture σ. The third type consists of either of the first two types, multiplied by a Kolmogorov spectrum $\Phi(u) = u^{-8/3}$. While the first

two types of "filter functions" serve to demonstrate the sensitivity of a given measurement to perturbations of various sizes, the third type gives a more realistic idea of the relative importance of various wavenumbers in a practical situation, where the refractivity spectrum is strongly biased toward large irregularities. The fourth type of "filter function" consists of the evaluation of the integral in question over all variables (including u) except s, position along the path. The result, plotted as a function of s, expresses the relative importance of different portions of the transmission path in the production of a given perturbation, assuming a uniformly random medium. A Kolmogorov spectrum is assumed.

The simplest and most well known "filter function" is that for the plane-wave, amplitude-covariance case, first given by Tatarski (1961, p. 149) for the case d = 0. It is shown in Figure 10.1 for three values of d. The quantity plotted is the evaluation of (2.15) over the variable s. The amplitude covariance is insensitive to small wavenumbers u, and the effect of high wavenumbers is reduced by increasing receiver separation d. The corresponding evaluation for phase-covariance is shown in Figure 10.2. It differs from the preceding case in that small wavenumbers are important; in fact, it is easily shown that those irregularities which are most effective in the production of amplitude fluctuations are least effective in the production of phase perturbations.

Another pair of amplitude- and phase-covariance "filter functions" is shown in Figures 10.3 and 10.4. In this case, the parameter is receiver aperture, and the relevant integral is (8.12), evaluated over s. Increased aperture has an effect similar to that of increased path separation, but is even more effective in reducing the importance of high wavenumbers, due to the rapid falloff of the Gaussian. Figures 10.5 and 10.6 differ from the preceding two only in that the results have been multiplied by $u^{-8/3}$, to simulate a typical spectrum $\Phi(u)$. The curve in Figure 10.5 for amplitude variance peaks at about $u\sqrt{L/k} = 1.6$, or for a period of the perturbation of $1.6\sqrt{\lambda L}$, in terms of the Fresnel zone radius. Contributions from higher wavenumbers decrease rapidly.

The effect upon the variance of amplitude can be easily seen, since variance is simply the area under the curves. Finite receiver aperture has less effect in the case of phase covariance, since large perturbations are most important. The area under the curves of Figure 10.6 is not finite for a $u^{-8/3}$ spectrum; in the atmosphere the spectrum ceases to increase with decreasing wavenumber at what is called the "outer scale," resulting in finite phase variance.

Spatial "filter functions" for amplitude and phase covariance are shown in Figures 10.7 and 10.8, a Kolomogorov spectrum being assumed (with an "outer scale" assumed in the case of phase covariance). Note that regions near the receiver (R in the figures) contribute little to amplitude fluctuations, and a maximum amount to phase fluctuations.

The "filter-functions" of other quantities are of interest, since they are potentially sensitive to different regions of the refractivity spectrum or different portions of the transmission path. That for amplitude-phase covariance (cf. (7.5)) is shown in Figure 10.9, and in Figure 10.10 is shown multiplied by a $u^{-8/3}$ spectrum. The "spatial filter function" for this quantity is shown in Figure 10.11. The "filter function" for angle-of-arrival covariance (cf. (7.4)) is shown alone in Figure 10.12, and with an assumed

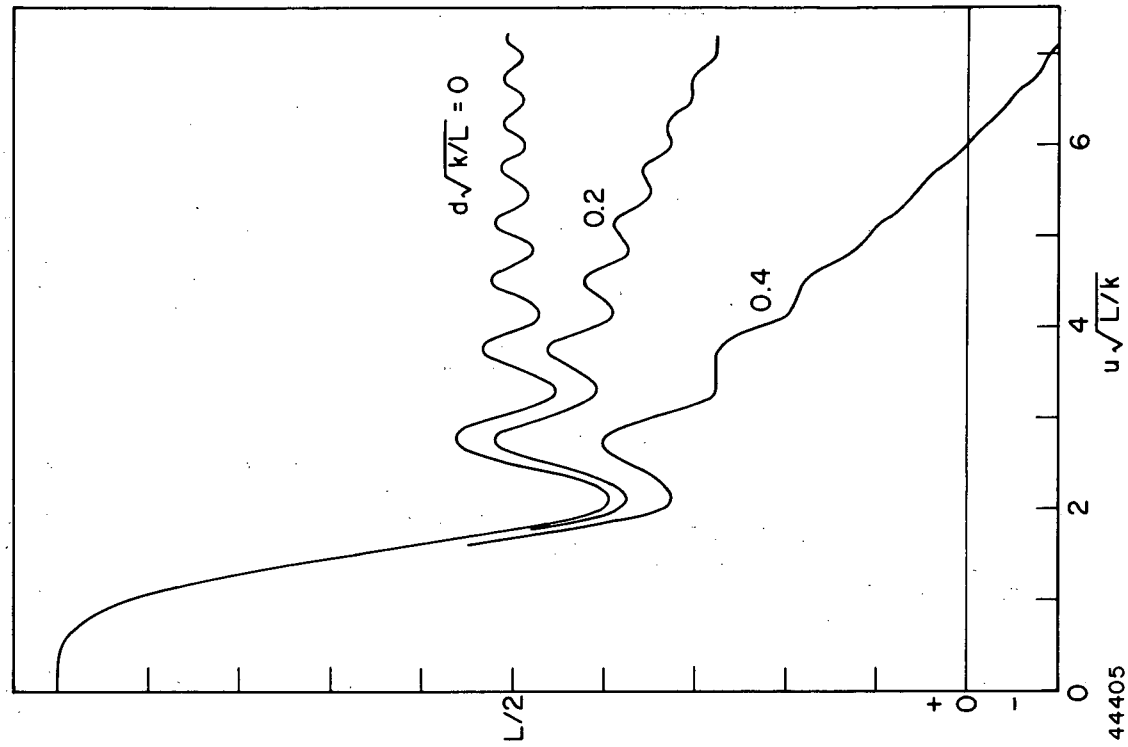

Figure 10.2. Plane-wave phase covariance "filter function" for three values of receiver separation.

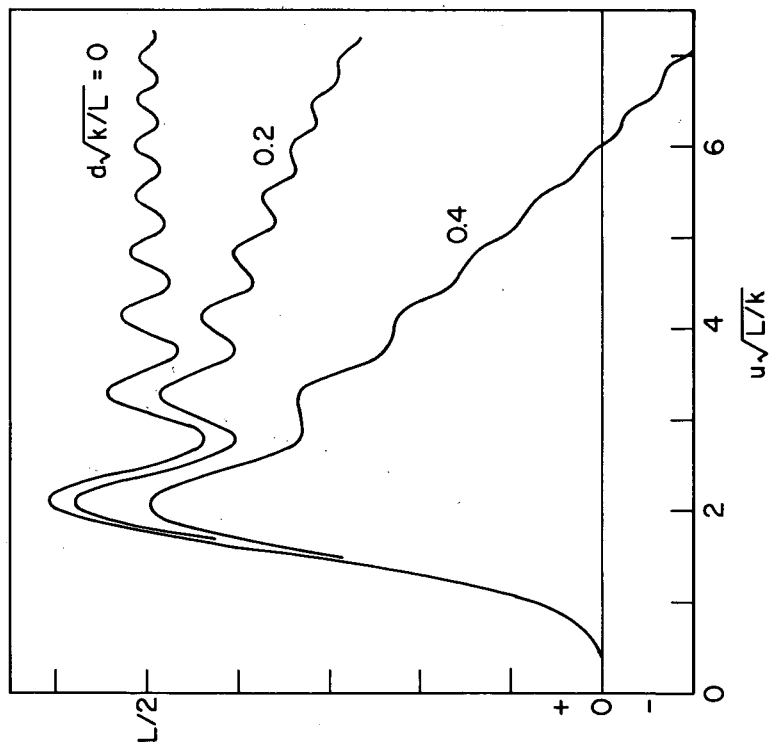

Figure 10.1. Plane-wave amplitude covariance "filter function" for three values of receiver separation.

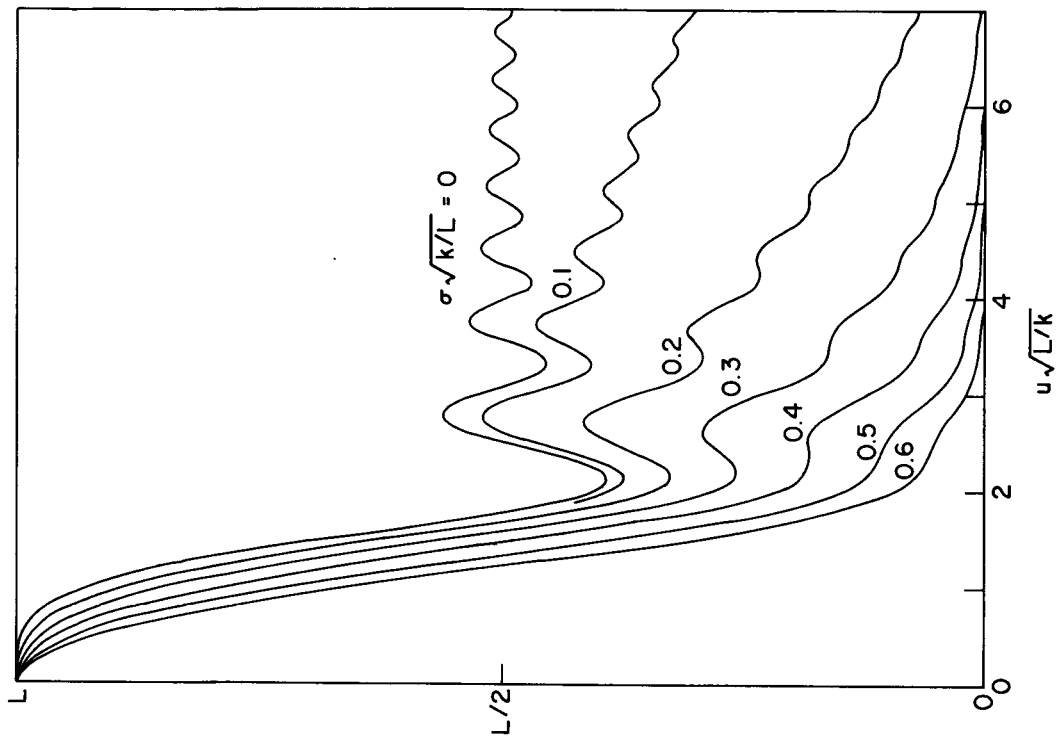

Figure 10.4. Plane-wave phase covariance "filter function" for several values of receiving aperture σ.

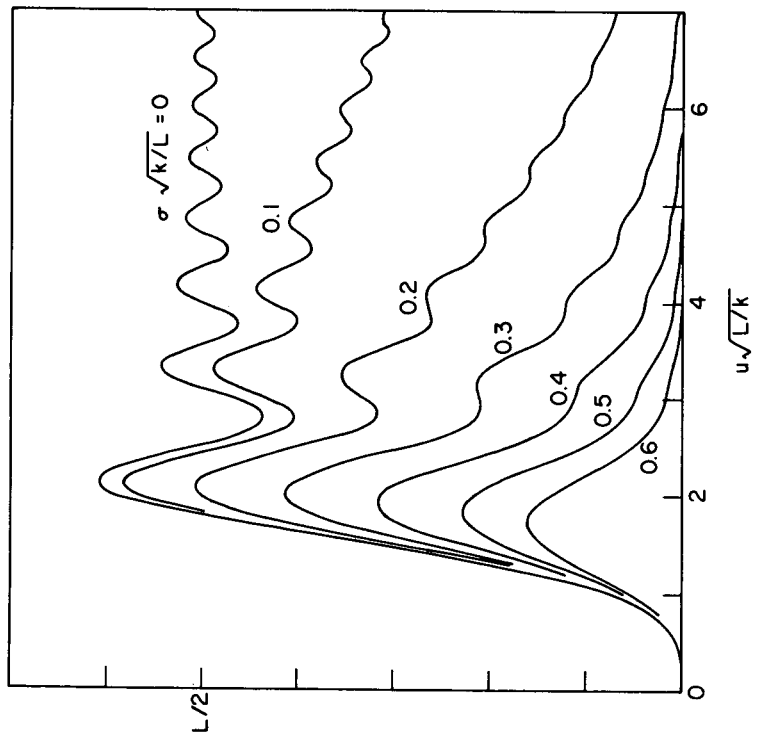

Figure 10.3. Plane-wave amplitude covariance "filter function" for several values of receiving aperture σ.

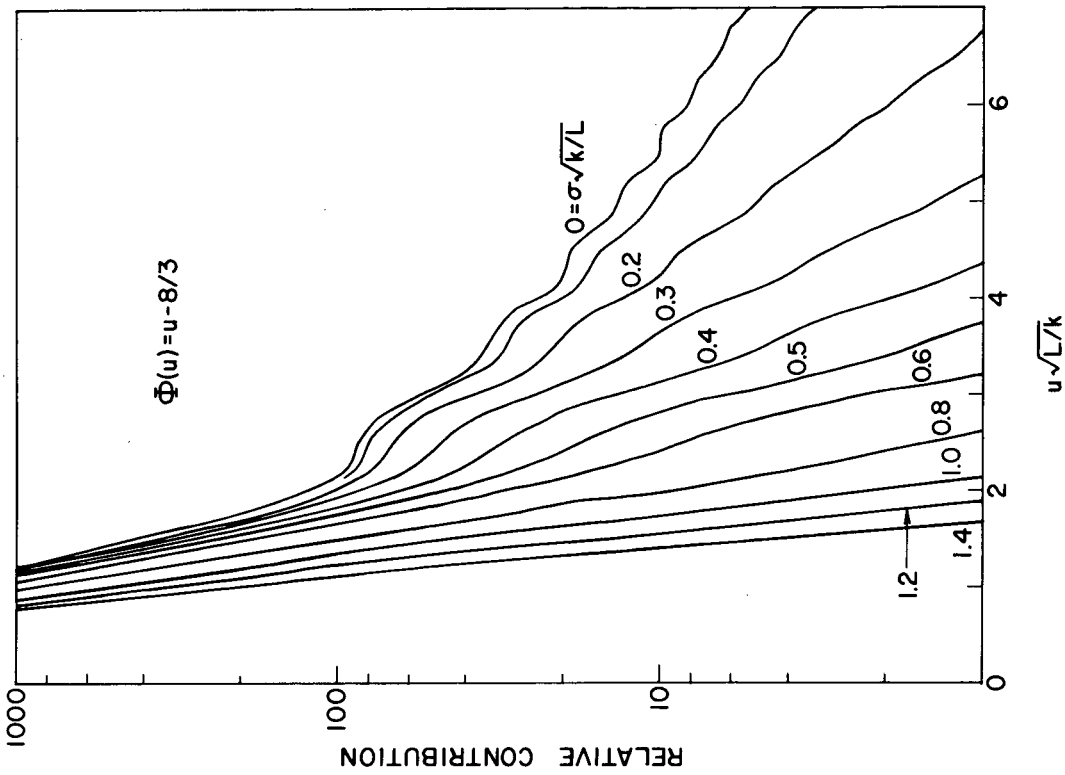

Figure 10.6. Plane-wave phase covariance "filter function" multiplied by $\Phi(u)$, for several values of receiving aperture σ.

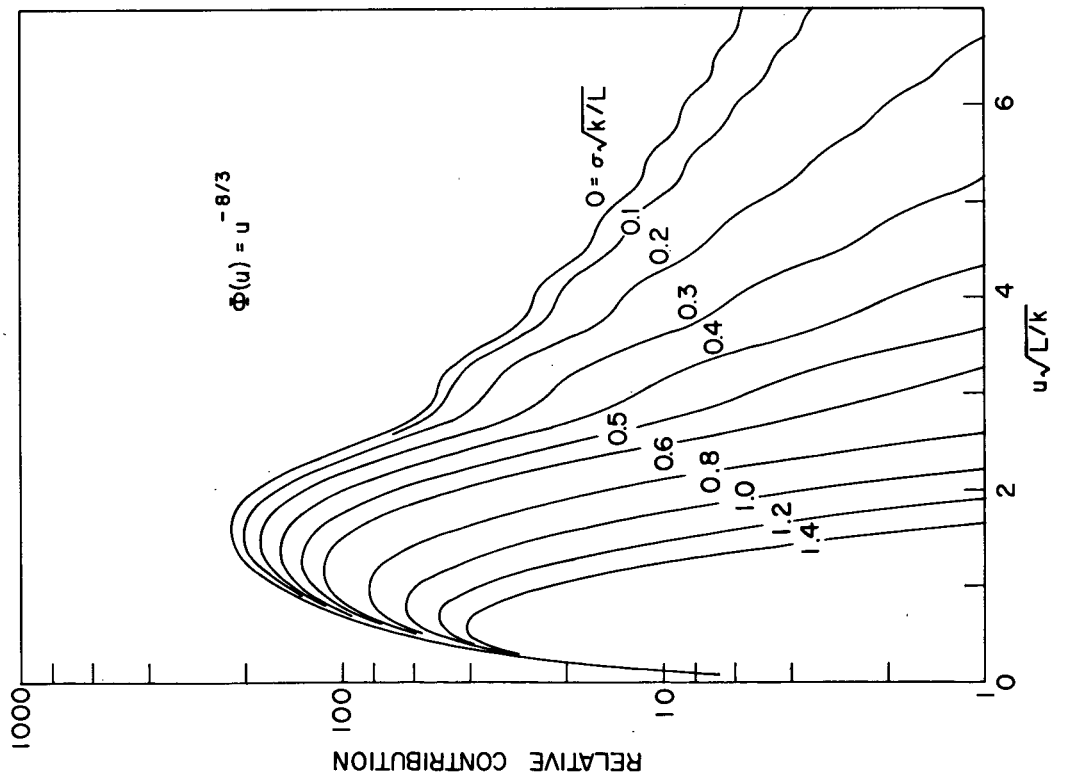

Figure 10.5. Plane-wave amplitude covariance "filter function" multiplied by $\Phi(u)$, for several values of receiving aperture σ.

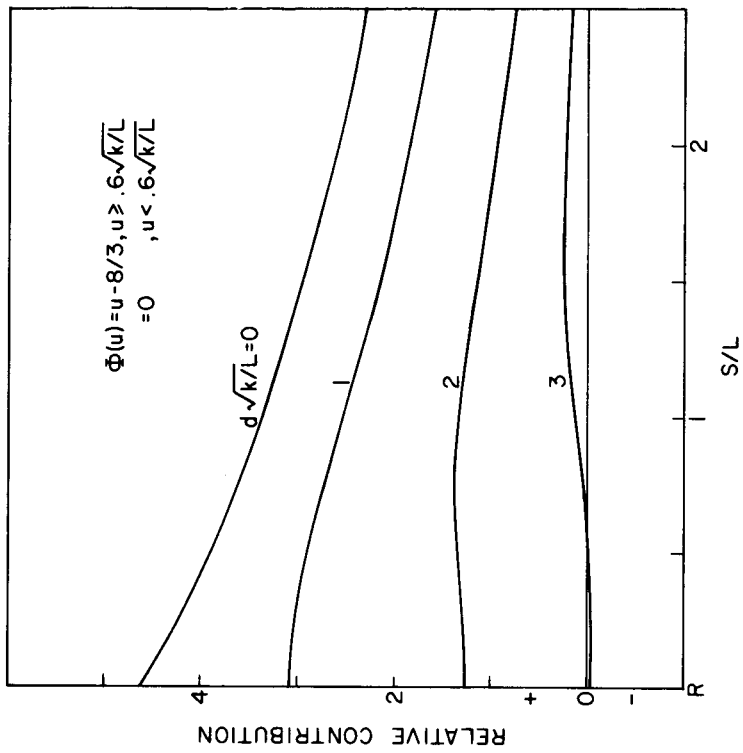

Figure 10.8. Plane-wave phase covariance "spatial filter function."

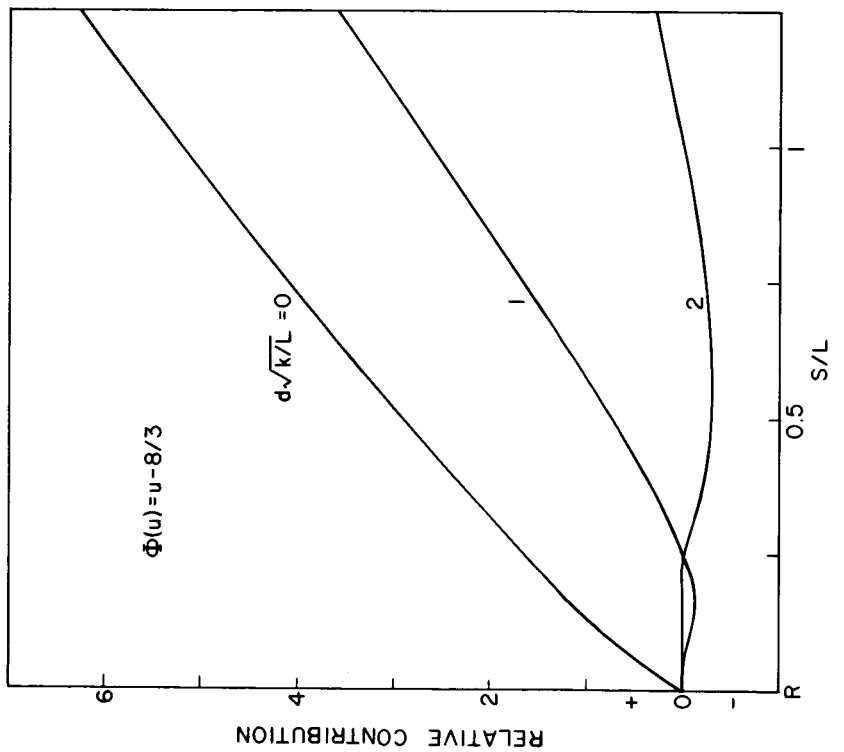

Figure 10.7. Plane-wave amplitude covariance "spatial filter function."

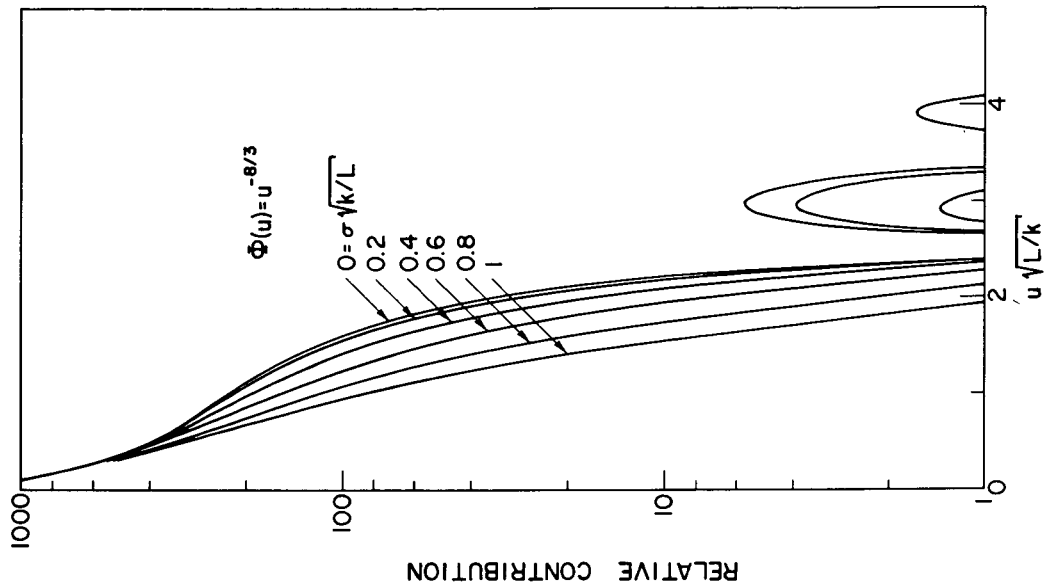

Figure 10.10. Plane-wave amplitude vs. phase covariance "filter function" multiplied by $\Phi(u)$, for several values of receiving aperture σ.

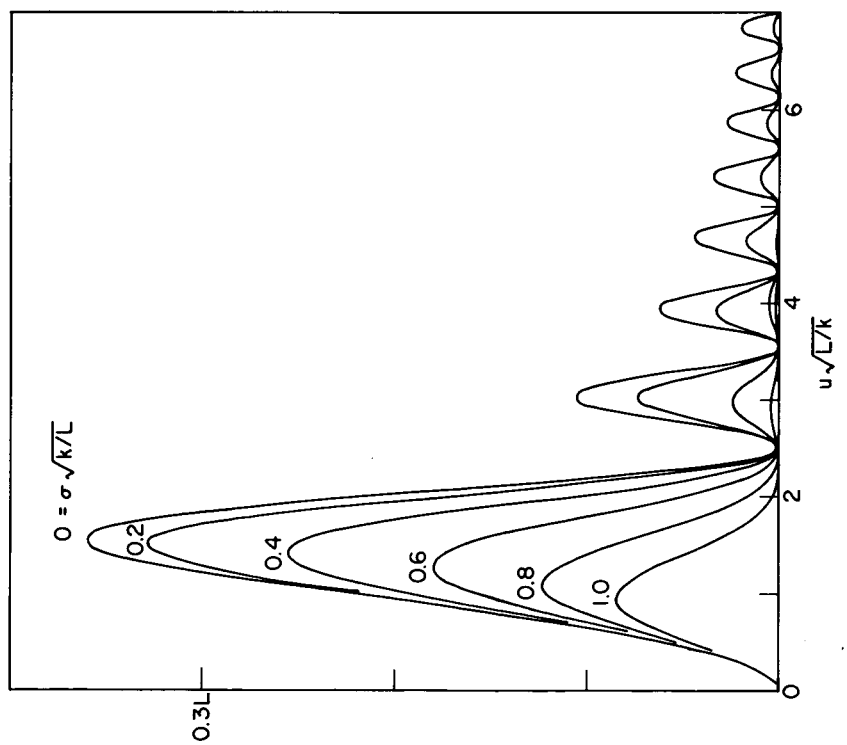

Figure 10.9. Plane-wave amplitude vs. phase covariance "filter function" for several values of receiving aperture σ.

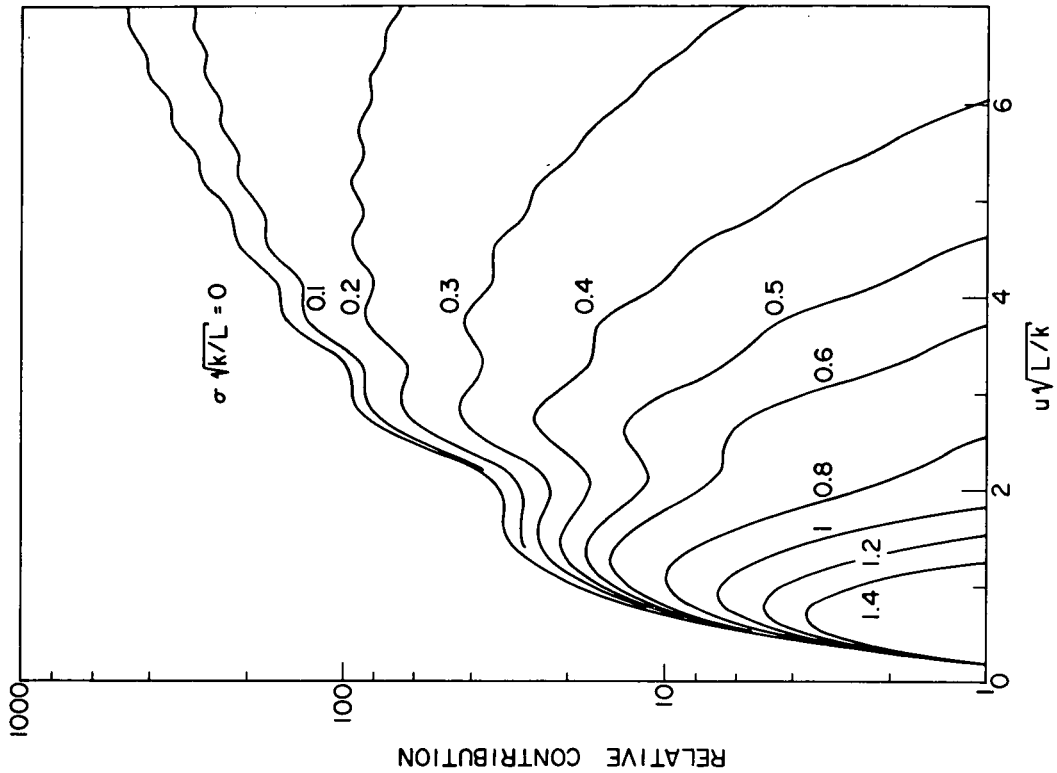

Figure 10.12. Plane-wave angle-of-arrival covariance "filter function" for several values of receiving aperture σ.

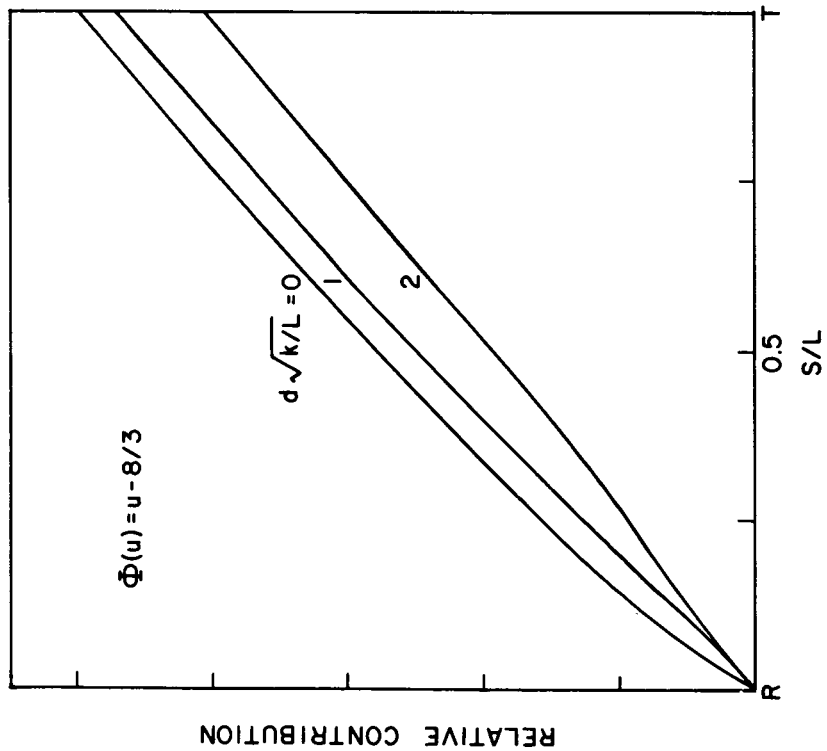

Figure 10.11. Plane-wave amplitude vs. phase covariance "spatial filter function."

spectrum in Figure 10.13. The "spatial filter function" is shown in Figure 10.14, where the case d = 0 is not shown. The variance is not finite for a $u^{-8/3}$ spectrum, unless the aperture or path separation is finite, or the spectrum terminates at some maximum wavenumber. There is no convergence problem at the low end of the spectrum in this case.

Thus far, plane wave situations have been considered. As an introduction to the spherical-wave geometry, attention is drawn to the basic amplitude-covariance integral (3.13). The "filter function" portion of this integral is the $\sin^2$ term, the zeroes of which are plotted as solid lines in Figure 10.15. Zeroes of the Bessel function in (3.13) are plotted as dashed lines. When a $u^{-8/3}$ spectrum is mentally superimposed upon Figure 10.15, the relative contributions can be imagined in two dimensions—in s and in u. It can be seen, for example, that the Bessel function serves to reduce the contribution of high wavenumber perturbations near the receiver (s/z = 1), while having little effect near the transmitter. Similarly, the $\sin^2$ term serves to emphasize large perturbations near mid-path, and smaller-scale perturbations towards the ends of the path. In quantitative terms, the $\sin^2$ term places major emphasis upon those perturbations which are equal in size to the Fresnel ellipsoid, which of course is small near the ends of the path and largest in the center. At high-wavenumbers the situation is very complex, some wavenumbers contributing negatively to the covariance, others positively and some not at all, since they are very poor scatterers.

Amplitude and phase-covariance "filter functions," as obtained from (3.13) by integration over s, are shown in Figure 10.16 for two values of d; they are rather similar to those in the plane wave case (Figures 10.1 and 10.2); finite receiver separation is quite effective in reducing the contribution of high-wavenumber perturbations. The same quantities, multiplied by an assumed spectrum, are shown in Figure 10.17, and the "spatial filter functions," obtained by integrating (3.13) in u (with an assumed spectrum), are shown in Figures 10.18 and 10.19. The peak of the amplitude-variance curve in Figure 10.17 occurs at $u\sqrt{L/k} = 3$, or for a period of the perturbation of about $0.8\sqrt{\lambda L}$, in terms of the Fresnel-zone radius (vis. $1.6\sqrt{\lambda L}$ in the plane-wave case), and of course contribution from high wavenumbers is greatly reduced due to the steep slope of the spectrum. Note in Figure 10.18 that increasing receiver separation tends to emphasize that portion of the path near the transmitter, and in any case the very ends of the path are unimportant. In the case of phase variance (Figure 10.19, d = 0), the whole path is almost equally important (for the outer-scale chosen; a smaller outer-scale would reduce the importance of mid-path).

As an example of another function, the "filter function" for amplitude-phase covariance is shown alone in Figure 10.20, and multiplied by an assumed spectrum in Figure 10.21. The "spatial filter function" is shown in Figure 10.22; it is similar to the amplitude-covariance case, but is less sensitive to increased receiver separation. The "filter function" for spherical-wave angle-of-arrival variance is shown alone in Figure 10.23, and multiplied by an assumed spectrum in Figure 10.24. As in the plane-wave case, this integral is not convergent for a $u^{-8/3}$ spectrum unless the aperture or separation is finite. Thus, in the "spatial filter function" shown in Figure 10.25, the case d = 0 is not given. Figure 10.25 is unique among the spherical-wave, "spatial filter functions" given here, in its emphasis upon the region near the receiver, and lack of emphasis near the transmitter.

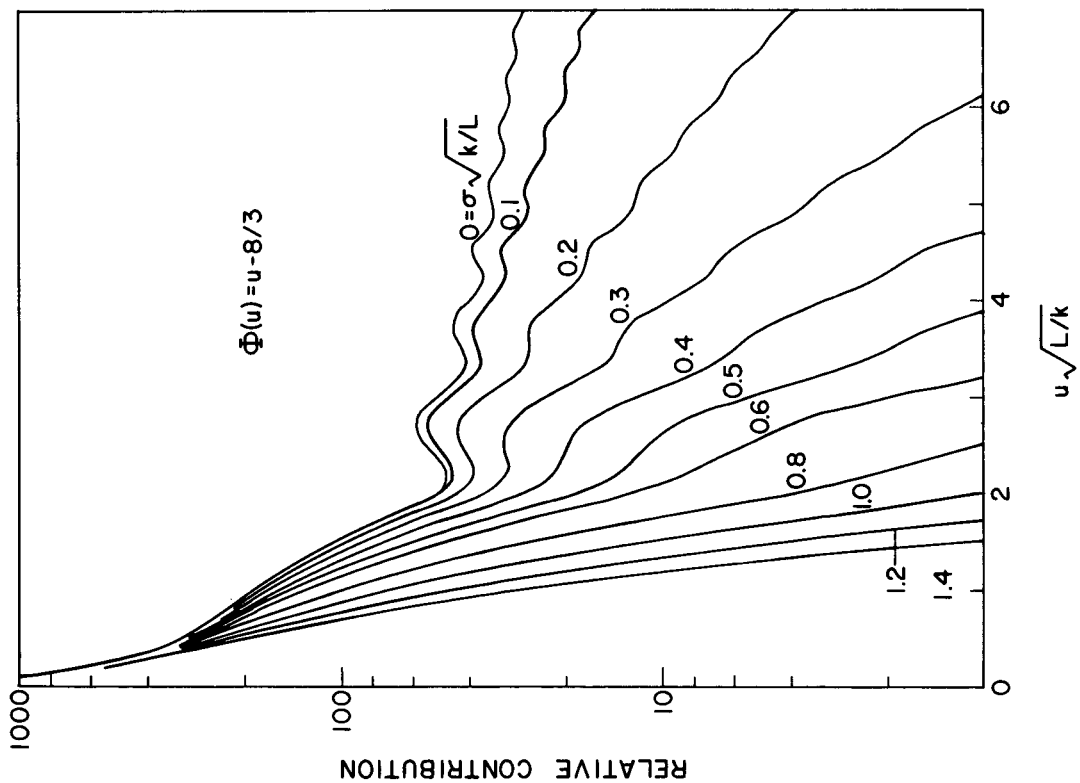

Figure 10.13. Plane-wave angle-of-arrival covariance "filter function" multiplied by $\Phi(u)$, for several values of receiving aperture σ.

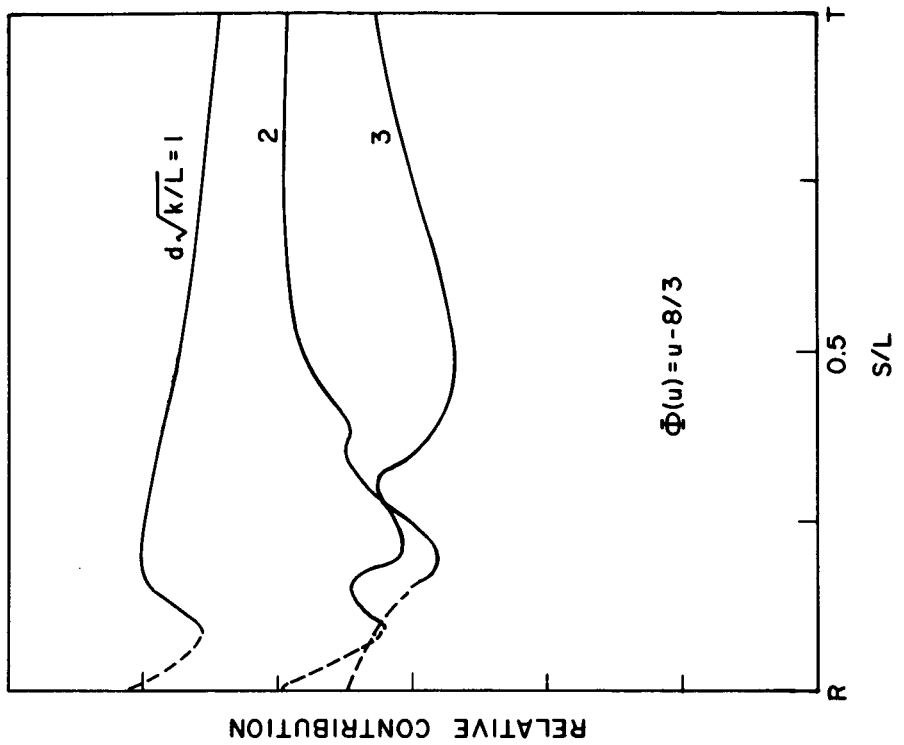

Figure 10.14. Plane-wave angle-of-arrival "spatial filter function."

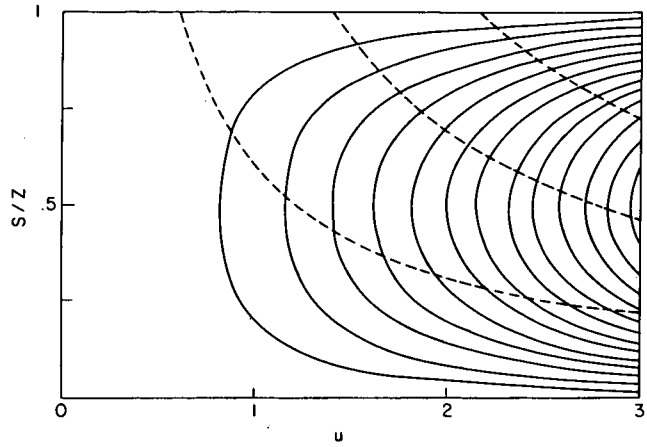

Figure 10.15. Zeroes of the function $J_0(dsu/L) \sin^2 (u^2 s(L-s)/2kL)$, with L = 28000, k = 716, d = 4.

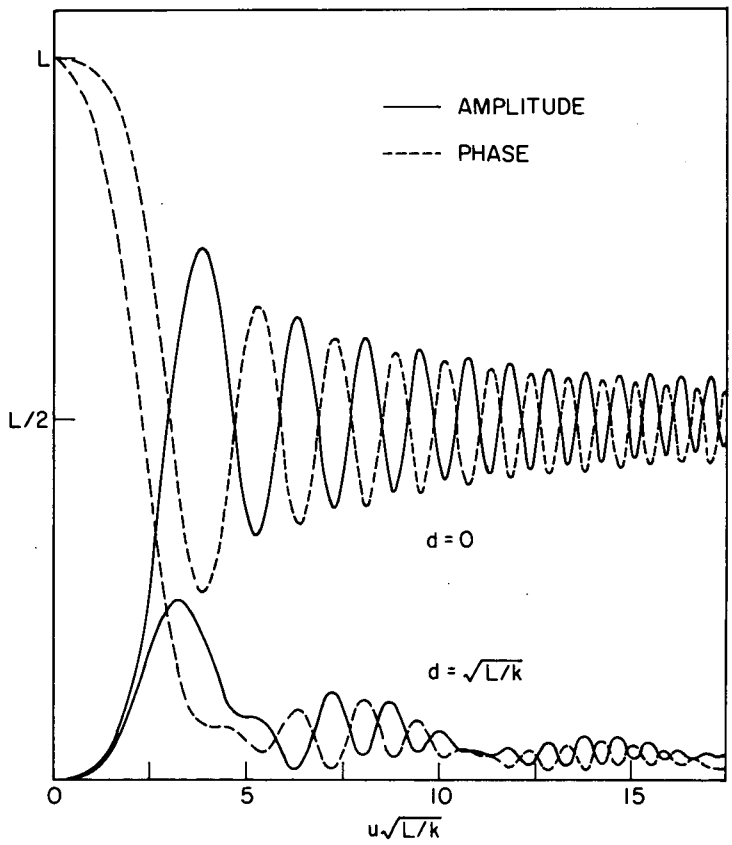

Figure 10.16. Spherical-wave amplitude and phase covariance "filter functions" for two values of receiver separation d.

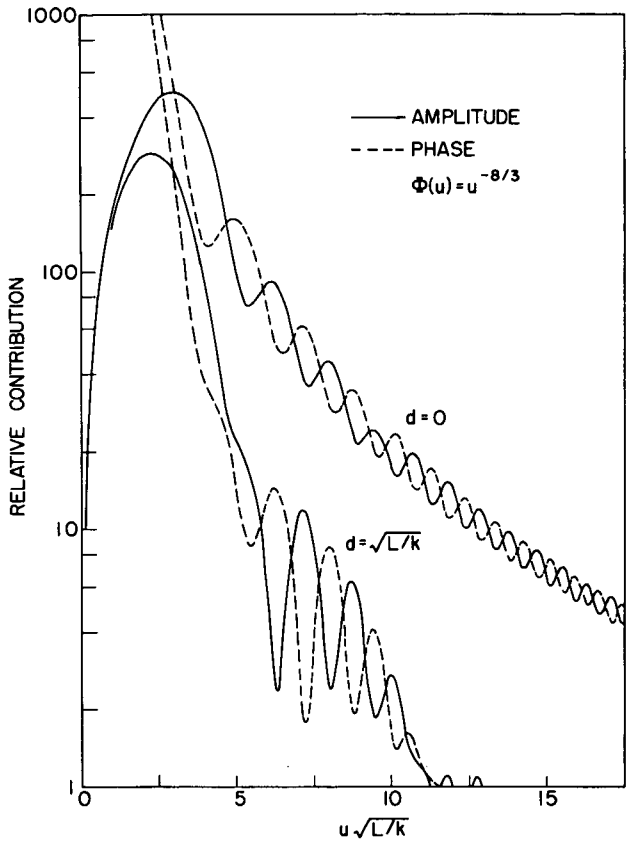

Figure 10.17. Spherical-wave amplitude and phase covariance "filter functions" for two values of receiver separation d.

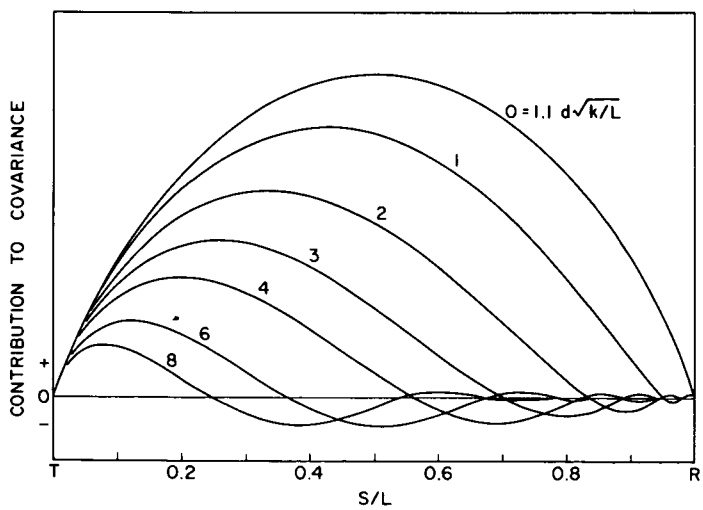

Figure 10.18. Spherical-wave amplitude covariance "spatial filter function."

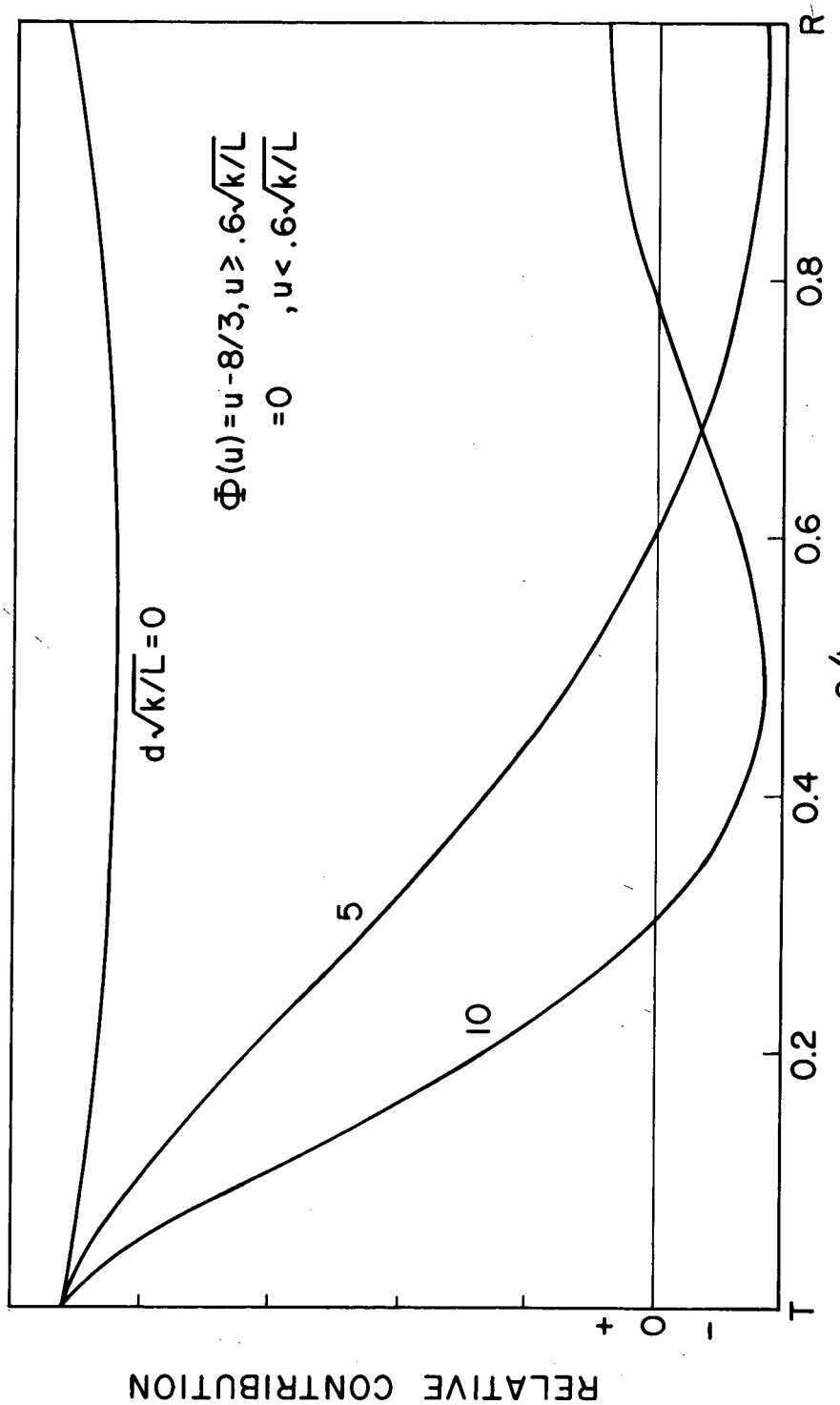

Figure 10.19. Spherical-wave phase covariance "spatial filter function."

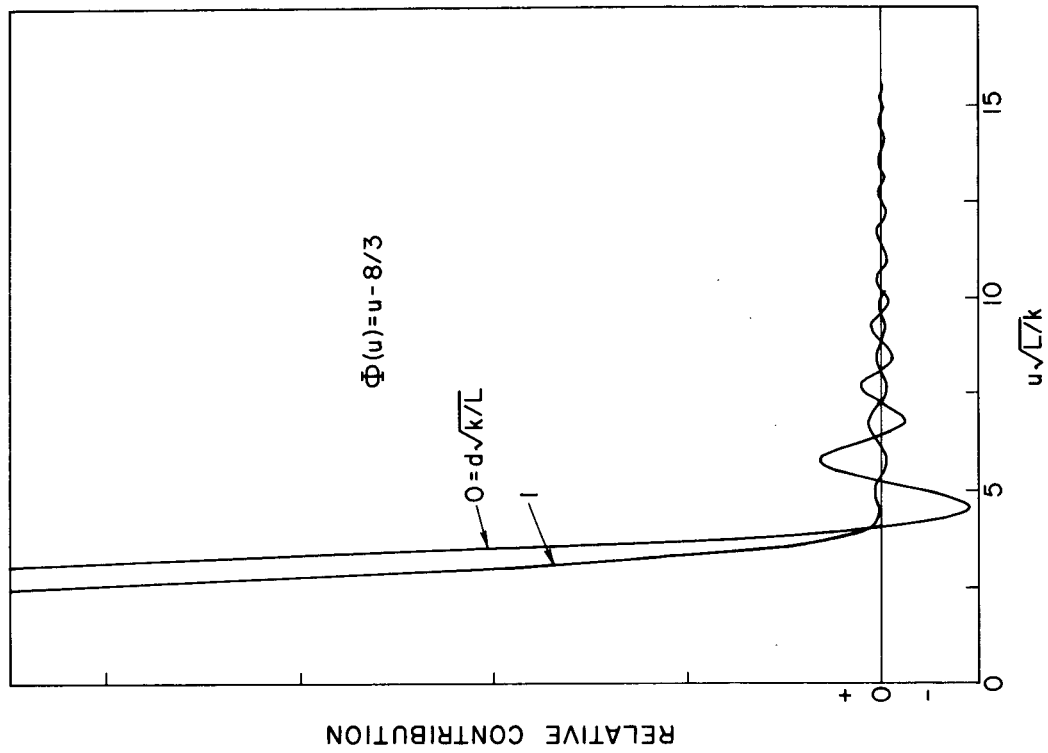

Figure 10.21. Spherical-wave amplitude vs. phase covariance "filter function" multiplied by $\Phi(u)$, for two values of receiver separation d.

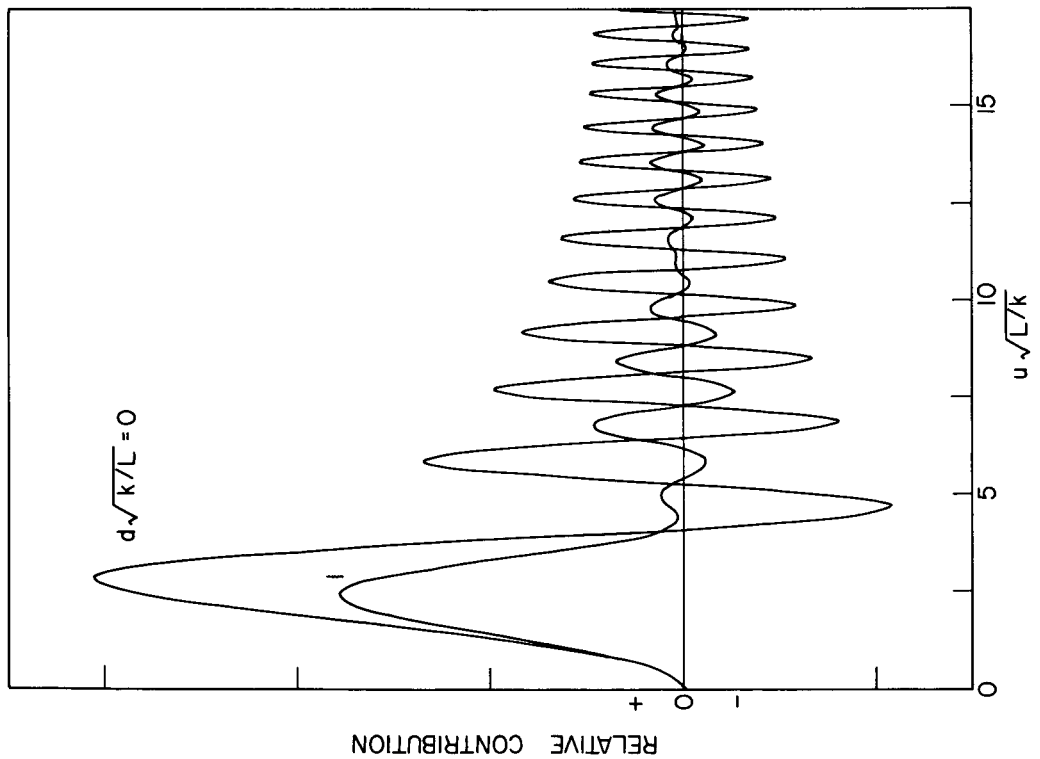

Figure 10.20. Spherical-wave amplitude vs. phase covariance "filter function" for two values of receiver separation d.

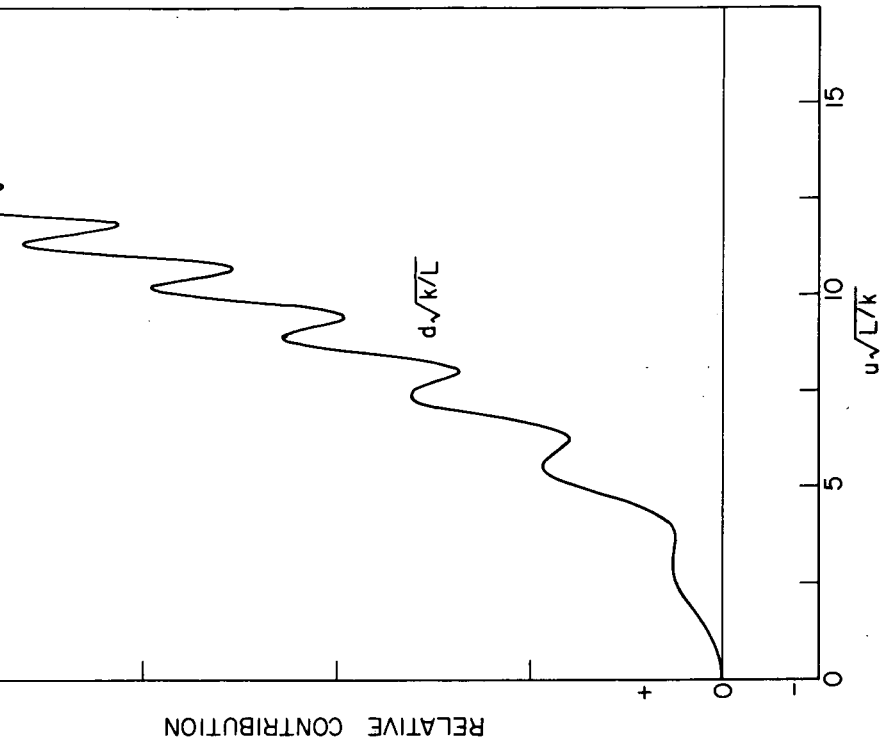

Figure 10.23. Spherical-wave angle-of-arrival covariance "filter function" for receiver separation d = 0.

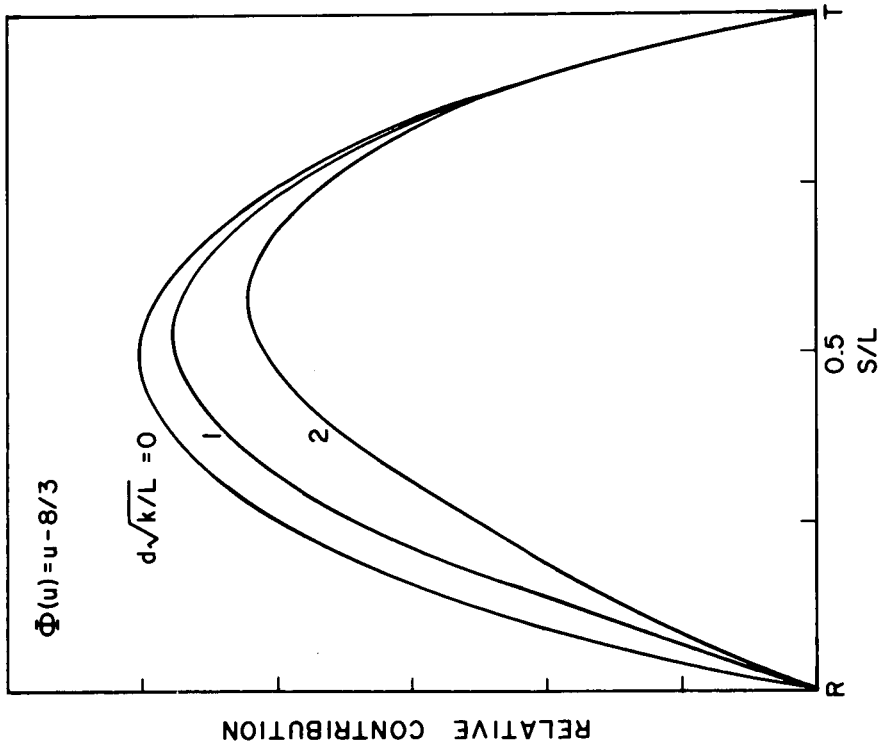

Figure 10.22. Spherical-wave amplitude vs. phase covariance "spatial filter function."

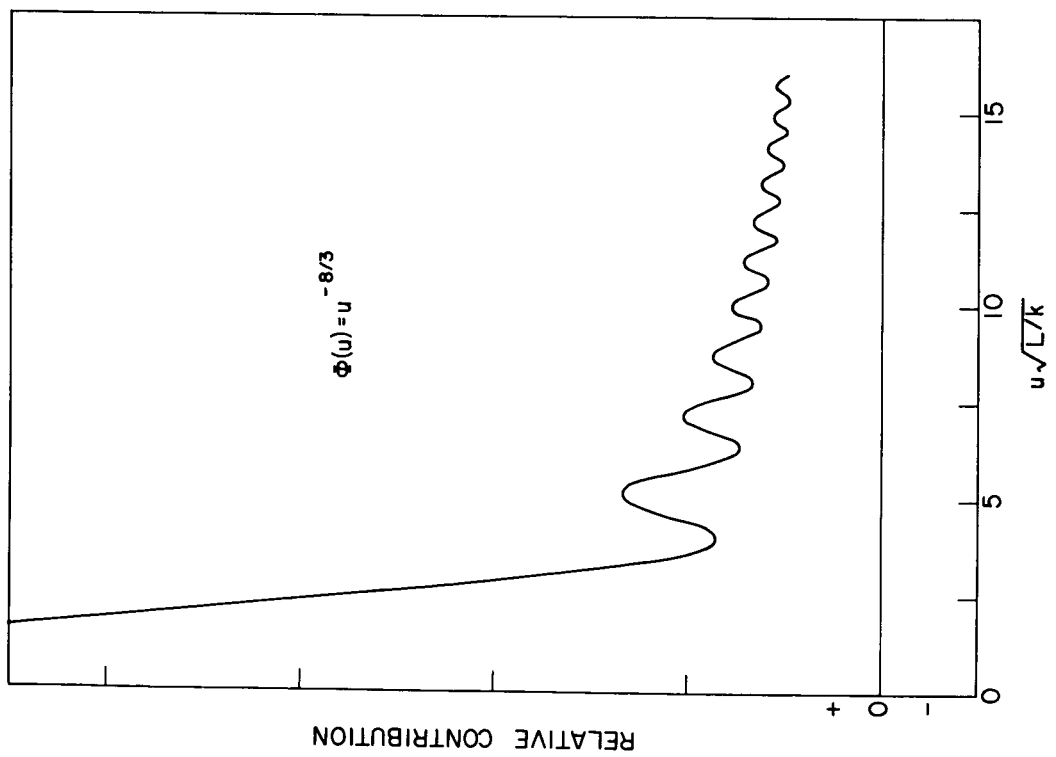

Figure 10.24. Spherical-wave angle-of-arrival covariance "filter function" multiplied by $\Phi(u)$, for receiver separation d = 0.

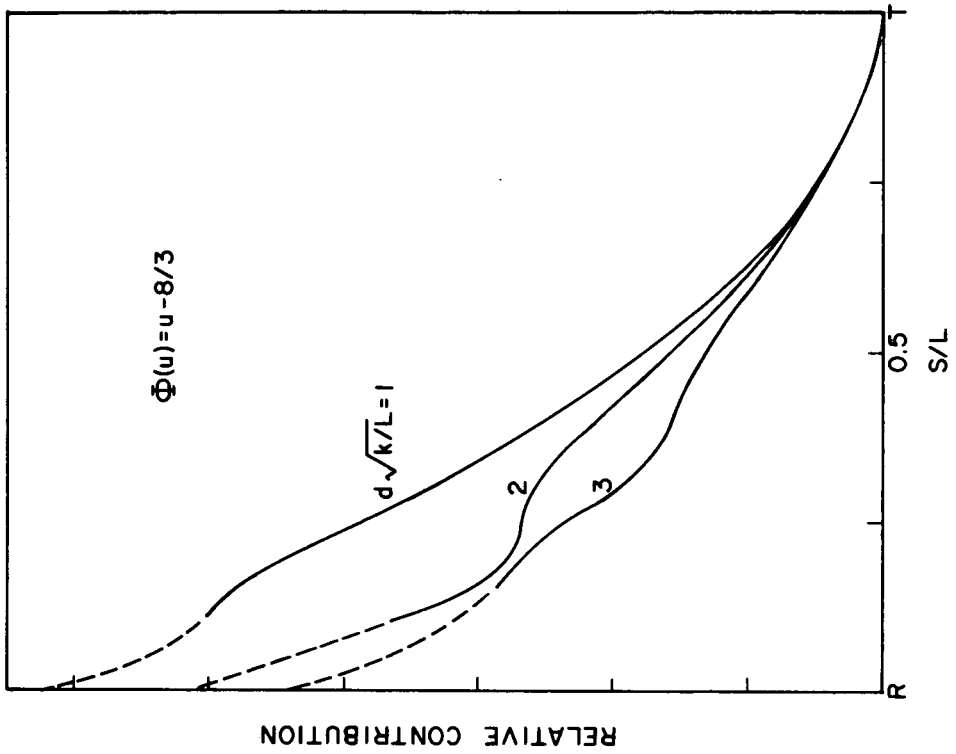

Figure 10.25. Spherical-wave angle-of-arrival covariance "spatial filter function."

These examples of "filter functions" demonstrate that, to some extent, the region of the medium or the range of wavenumber of interest can be emphasized by proper choice of the quantity measured. Perhaps more importantly, they also demonstrate that conclusions based upon measurements are valid only over a certain range of wavenumbers, or perhaps over a certain portion of the transmission path.

11. THE USE OF PROPAGATION MEASUREMENTS IN ATMOSPHERIC PROBING

Considerable interest exists in the application of microwave and optical propagation measurements to the determination of various atmospheric parameters, both because such measurements can be made without actually placing an instrument at the point of measurement, and because the potential exists for measuring quantities otherwise very difficult to measure at all. The basic problems involved in relating propagation measurements to atmospheric parameters are three. First, a suitable analytical framework must be developed, expressing the relationship between the parameter of interest and the measurements; this has been the subject of the preceding sections of this report. Secondly, measurements of sufficient quality must be obtained. Finally, suitable mathematical techniques must be used to obtain from the measurement the desired information about the atmosphere. This latter problem is not trivial; the expressions derived in the preceding sections equate the measured quantity with an integral over atmospheric parameters, and thus the problem is to solve an integral equation (and generally a family of such equations). In only a few of the cases of interest is it possible to invert the integral analytically and we shall generally be forced to use iterative, numerical techniques.

Atmospheric parameters of interest may be conveniently divided into two categories—quantities averaged over the transmission path, and quantities about which spatial information is desired. The simplest quantity of the first type is the magnitude of the refractivity spectrum, C_n^2. This quantity may be obtained simply by measuring the variance of the amplitude of the received signal. It must be borne in mind, however, that this quantity as measured is a weighted average—weighted along the path and weighted in wavenumber u, as described by the "filter functions" plotted in Section 10. Thus, if the refractivity spectrum is not uniform along the path, or is not of the form assumed (Kolmogorov, for instance), the results will be difficult to interpret. A more sophisticated approach to measuring the magnitude of the refractivity spectrum is to consider the form of the spectrum to be unknown, and solve for the form as well as the magnitude (assuming spatial uniformity of the spectrum). To take a simple case, consider plane-wave amplitude covariance, as governed by (2.13). Rewriting that expression,

$$C_a(d) = \int_0^k du\, u\Phi(u)\, J_o(du) \int_0^L F(u,s)\, ds \tag{11.1}$$

where $\Phi(u)$ is the unknown quantity, and $C_a(d)$ the measured quantity. This expression can be inverted explicitly as a Hankel transform.

$$u\Phi(u) = \int_0^\infty d' J_o(d'u) C_a(d')\, dd' \Big/ \int_0^L F(u,s)\, ds \tag{11.2}$$

Similar analytical inversions are possible in the spherical-wave case, but only for parallel-path situations (where the variable s does not appear in the argument of the Bessel function). Such a situation occurs in the case of time-covariances, when the windfield is uniform. Covariance is then measured as a function of Vt, rather than d, and the inversion proceeds in the same fashion as above. In the general spherical-wave situation, analytic transformation is not possible, but simple numerical techniques are available. For instance, the spectrum, $\Phi(u)$, can be assumed to have some form—as a series of step functions in s with unknown amplitudes at each step. The covariance at each separation d can then be written as a summation of integrals over the various steps in s, the whole set then forming a family of linear simultaneous equations. This is easily solved, and n measurements of covariance provide n degrees of freedom in the result.

Such measurements and subsequent transformations have proved to be of great value at the upper limit of the refractivity spectrum where, with very short optical paths, it is possible to measure the rather sharp cutoff of the spectrum. It should be equally valuable to examine the lower end of the spectrum where the suitable technique would be (as can be seen from the filter functions in Section 10) measurements of phase covariance over parallel paths. It would also be of interest to investigate the "inertial subrange" for departures from the expected Kolmogorov spectrum. Here the appropriate tool would be millimeter-wave amplitude covariance measurements.

As an example of another more-or-less spatially averaged quantity, wind velocity can be measured to a degree by correlation techniques. It can be seen from (6.2) that the time-lag for which the time-autocorrelation function (d = 0) falls to a given value is inversely proportional to the velocity V. In Figure 11.1 is plotted the reciprocal half-width of the amplitude time-correlation function, vs. time, as observed on the array described previously (Lee and Waterman, 1966). This quantity should thus be proportional to the velocity, and that it is to a degree can be seen by comparison with Figure 11.2, taken from measurements made 250 m under the propagation path.

We now consider the second category mentioned above, quantities whose spatial distribution is to be studied. The simplest such quantity is the magnitude of the refractivity spectrum, C_n^2. In either the plane- or spherical-wave case we are faced with a linear integral equation of the first kind. We proceed as before, and assume that C_n^2 is a series of step functions in s, and the amplitude of the several steps is unknown. A family of linear, simultaneous equations results, the solution of which furnishes the desired dependence of C_n^2, with the resolution dependent upon the number of measurements available.

The above examples are relatively simple, and present no mathematical problems, but are nevertheless quite useful. As a final example, we will consider a much more difficult problem, that of determining windspeed as a function of position s.

As can be seen from (6.2), velocity appears in the argument of the Bessel function which is always present in the covariance integrals. Thus the problem is that of inverting a family of non-linear integral equations, rather than linear integral equations. The general techniques for solution remain the same—assuming a form for the solution, with unknown parameters, and then solving a set of simultaneous equations for those parameters.

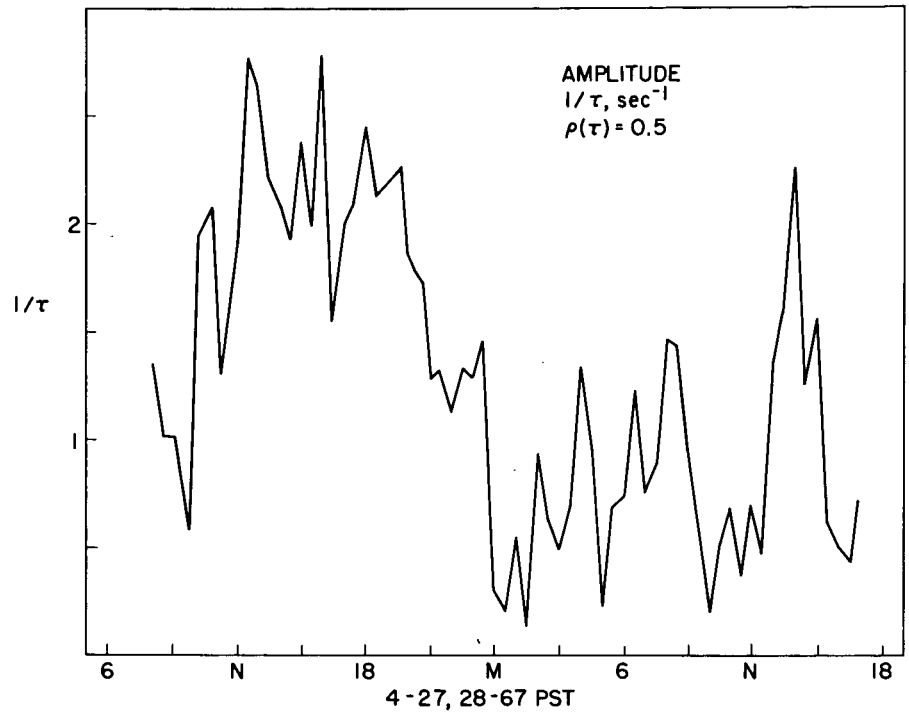

Figure 11.1. Reciprocal half-width of amplitude time-correlation function, as measured on April 27/28, 1967.

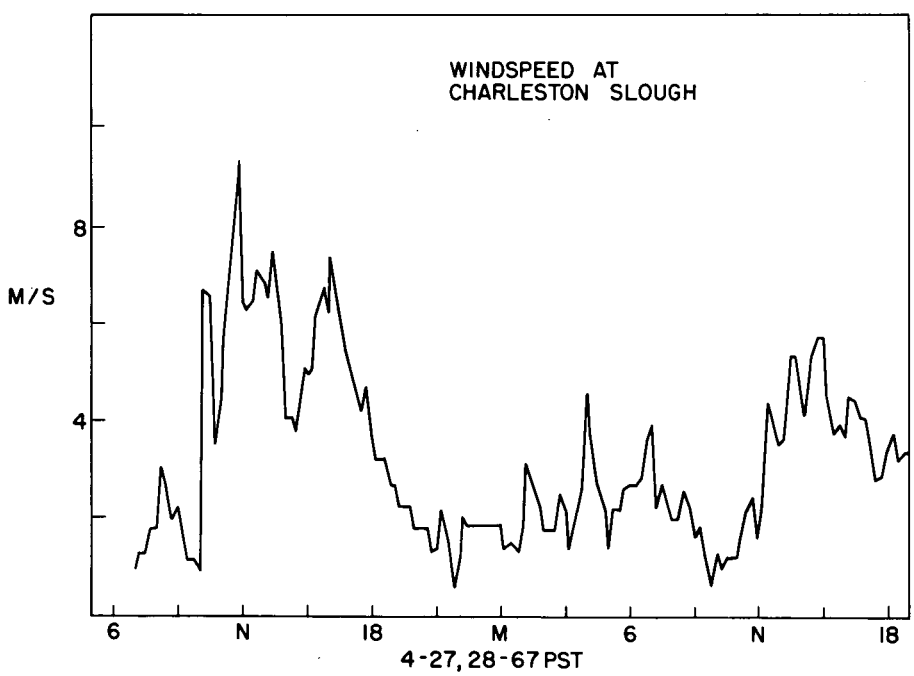

Figure 11.2. Surface wind velocity measured near mid-path on April 27/28, 1967.

In the general case of non-linear integral equations, however, these simultaneous equations are themselves non-linear, and therefore must be solved by iterative numerical techniques. While such solutions are not difficult in principle, they are mathematically messy, and certain techniques can be used to simplify the process, at the expense of some detail in the results. One such technique is to linearize the integral involved by differentiation. The time-derivative of the time-lagged amplitude covariance function (plane-wave) is of the form

$$C'(d,O) = \int_O^k u^2 \Phi(u)\, J_1(du)\, du \int_O^L V(s)\, F(u,s)\, ds \qquad (11.3)$$

as evaluated at $t = 0$. Note that this is a linear equation of exactly the type considered earlier, and the solution follows the same lines. $V(s)$ may, for instance, be obtained as a stepwise-linear function of s, with as many steps as measurements. Information is lost in the process of differentiation—that information obtained at larger time-lags—and thus resolution is reduced. This information may be utilized by considering higher derivatives of the correlation function, still evaluated at $t = 0$. The set of simultaneous equations resulting from measurements of the second derivative are equations in $V(s)^2$, for example; that is, they are linear equations in $V(s)^2$. This process may be carried to still higher derivatives, until the derivatives are no longer meaningful. In practice, the measured time-lagged correlation functions would be fit to high-order polynomials, and the derivatives of these polynomials taken, thus making use of large time-lag covariances. Other techniques for solution exist, and may be exploited, but in general, simultaneous equations of even higher complexity (including cross-terms between the unknowns) result.

There are other problems involved in the interpretation of measurements along the lines suggested above, which deserve mention here. In the first place, such transformations are by nature sampled-data processes. Measurements are made at a finite number of points, separated in time and distance by finite increments. Hence the results obtainable from such transformations are subject to inherent limitations of resolution and region of validity. For example, in the determination of the spectrum $\Phi(u)$ by measurement of the spatial-covariance function and subsequent transformation, a lower-limit upon the separation in u of the resulting independent estimates of the spectral density is imposed by the maximum separation d available. This limit is easily derived, and is of the order $2\pi/d_{max}$. Similarly, an upper limit is set upon u by the smallest separation, of order $2\pi/d_{min}$. Energy from higher wavenumbers will "fold over" and contaminate estimates for lower wavenumbers. This process is exactly analogous to spectral analysis of time-sampled data. The accuracy of the resulting spectral-density estimates is also limited by the width of u included in the estimate ("bandwidth")—the narrower the bandwidth, the greater the statistical fluctuation of the spectral density estimates.

The second problem concerns the sensitivity of the measurement to the atmospheric parameter being estimated. Taking as an example the transformation (11.2), the quantity in the denominator can be recognized as the "filter function" appropriate to the measurement. If the measurement is relatively insensitive to the desired parameter (as very large or very small u in the case of amplitude covariances), the filter function is quite small, and its inverse quite large. Uncertainties in the measured quantity then become

very important, and the process is quite "noisy." Thus care must be exercised in choosing the range over which the unknown quantity is to be estimated.

A final problem concerns noise present in the measurements or generated in subsequent analysis. This noise can arise from several sources—finite signal-to-noise ratio, lack of stationarity in the atmosphere, and round-off errors in the mathematical transformation, to name a few. The effect of such noise sources can be estimated by propagating artificial errors through the transformation process.

Optimum solution of these problems is a difficult task, but general principles can be stated. Clearly, as many spacings and time-lags as possible should be used. It is highly desirable to over-constrain the unknowns, and obtain a least-squares solution, to reduce the effects of noise. By the same token, it is desirable to allow as few unknowns as possible, to enhance their statistical significance. To achieve this to the highest degree possible, full use should be made of all a priori knowledge concerning the medium, so that the assumed form of the solution may be tailored so as to require a minimum number of degrees of freedom. For example, if it is known that a certain quantity varies more rapidly near the termini of the path, the assumed step-function-series solution for this quantity should have broader steps near mid-path than at the ends. Such tailoring should not be carried too far, however, as there is danger of forcing a solution of the desired type.

12. CONCLUSION

The theory of line-of-sight propagation in random media, to which much of this report has been devoted, appears to be reasonably adequate for application to the determination of atmospheric parameters. It should be noted, however, that the theory cannot handle such non-random atmospheric phenomena as sharp layers or refractivity gradients, nor can it handle other than weak-scattering situations (such as long optical paths).

Experimental techniques are advancing rapidly, and have reached the point where the transformation techniques described above can be attempted. By far the most promising systems—and the only systems which provide the requisite number of separations required in the transformations—are arrays of receivers, sampling the received wave at several points in space simultaneously. Such arrays in the centimeter and millimeter region exist at Stanford, measuring both the phase and amplitude of the wavefront, and are contemplated or under construction elsewhere in both the microwave and optical regions.

Mathematical techniques exist for the transformation of the measurements in terms of atmospheric parameters. The quantities measured must be selected carefully, bearing in mind their sensitivity to variations of the parameters of interest, as evidenced by "filter functions." The statistical and other limitations inherent in the process must be considered, and maximum use should be made of available information about the medium, to reduce the number of unknowns in the problem. Finally, all assumptions regarding the refractivity spectrum, stationarity, isotropy, etc., must be regarded as suspect until and unless they can be justified by actual measurement.

This work is supported by AFCRL contract F04701-68-C-0110.

BIBLIOGRAPHY

Fried, D. L., 1966: J. Opt. Soc. Am., 56, 1380.

Fried, D. L., 1967: J. Opt. Soc. Am., 57, 175.

Hodara, H., 1966: Proc. IEEE, 54, 368.

Ishimaru, A., 1968: Amplitude fluctuations of a beam wave in a locally homogeneous medium, presented at 1968 Spring URSI, Washington, D.C., April 11, 1968.

Lee, R. W. and Waterman, A. T., 1966: Proc. IEEE, 54, 454.

Lee, R. W. and Harp, J. C., To be published in 1969.

Schmeltzer, R. A., 1967: Quart. Appl. Math., 24, 454.

Strohbehn, J. W. and Clifford, S. F., Private communication.

Tatarski, V. I., 1961: Wave propagation in a turbulent medium, McGraw-Hill Book Company, New York.

Taylor, G. I., 1938: Proc. Roy. Soc. London, Ser. A, 164, 476.